HetP and its three homologues: regions necessary for function of HetP and requirement of homologues for fixation of nitrogen in the filamentous cyanobacterium *Anabaena* sp. strain PCC 7120

A Thesis Submitted to the Graduate Division of the University of Hawai‘i at Mānoa in Partial Fulfillment of the Requirements for the Degree of

Master of Science

in

Microbiology

August 2013

By

Kathryn Lynn Hurd

Thesis Committee:

Sean Callahan, Chairperson

Paul Patek

Hongwei Li

ACKNOWLEDGEMENTS

I would like to thank Dr. Sean Callahan for the continued guidance in my education and research. I would also like to thank my lab members I have worked with over the past years: Silvia Beurmann, Andy Burger, Dr. Loralyn Cozy, Amanda Shore-Maggio, Orion Rivers, Chris Runyon, Sasa Tom, Blake Ushijima, Patrick Videau, and Jasmine Young

TABLE OF CONTENTS

LIST OF TABLES

LIST OF FIGURES

CHAPTER 1. INTRODUCTION

Anabaena as a Developmental Model

The filamentous cyanobacterium *Anabaena* sp. strain PCC 7120 is a Gram-negative prokaryote that performs oxygenic photosynthesis. In addition to being an obligate phototroph, *Anabaena* is capable of differentiating specialized nitrogen-fixing cells called heterocysts. The development of terminally-differentiated heterocyst cells occurs in the absence of fixed nitrogen and forms a one-dimensional pattern along the filament of vegetative cells. The exchange of intercellular signals controls the regulated spacing of the heterocyst cells that on average arise every tenth cell along the filament (Figure 1). The formation of heterocyst cells effectively separates the oxygen-labile nitrogenase complex from oxygen-evolving photosynthesis that occurs in vegetative cells. Heterocysts and vegetative cells are mutually interdependent. Heterocyst cells lack photosystem II and the capacity to fix carbon and must rely on the vegetative cells for sources of reductant. In return, heterocysts supply the filament with fixed nitrogen (Cumino et al. 2007; Marcozzi et al 2009). The development of two distinct cell types in a simple one-dimensional pattern makes *Anabaena* a simple example of cellular differentiation and pattern formation.

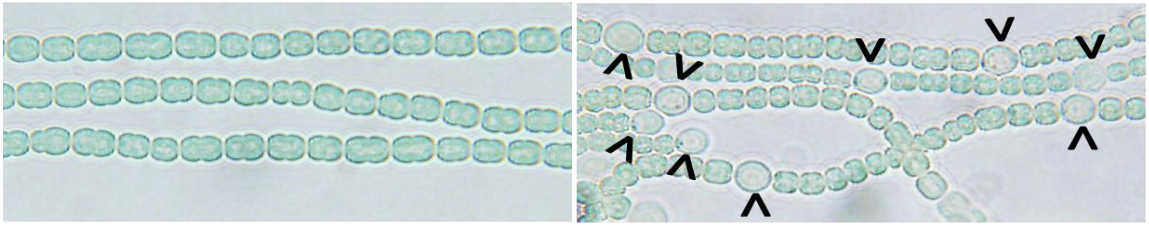

Figure 1: *Anabaena* sp. PCC 7120 grown with (left) and without (right) a source of fixed nitrogen. Heterocysts are indicated with carets.

Heterocyst differentiation may be considered a simple developmental system when compared to higher organisms; however, much of the differentiation process has yet to be elucidated. The process of heterocyst differentiation is comprised of four distinct stages: induction, pattern formation, commitment, and morphogenesis. Each of these stages is regulated by a complex genetic network. A general working model has been established to provide an overview of this complex process (Figure 2).

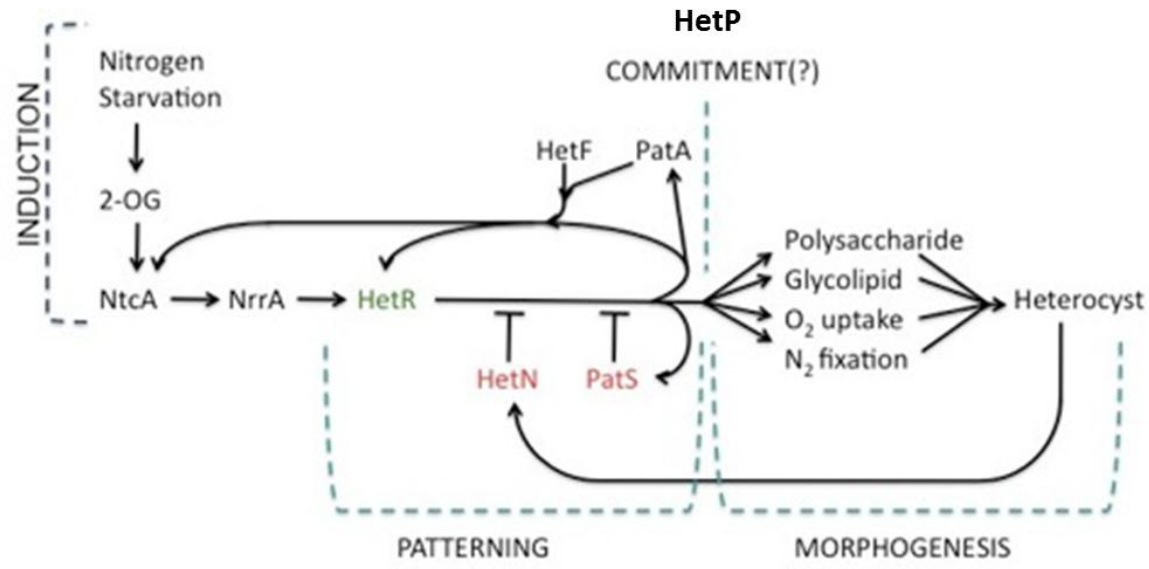

Figure 2: Model of the genetic network regulating heterocyst differentiation

Induction and Patterning of Heterocyst Differentiation

Induction of differentiation is triggered by a lack of fixed nitrogen in the environment. Ultimately, this process leads to activation of the protein HetR. HetR is known as the master regulator of cellular differentiation because its expression is both necessary and sufficient to drive heterocyst formation (Buikema and Haselkorn 1991a; Buikema and Heselkorn 2001). Null mutants lacking *hetR* fail to make heterocysts and the overexpression of *hetR* results in excessive production of heterocysts. HetR is positively auto-regulated (Black et al, 1993) and has been shown to bind DNA (Huang et

al, 2004). Certain key genes of heterocyst differentiation, including *hetP*, have been shown to have a HetR-binding site in the promoter region (Higa and Callahan, 2010). Mutations that block the DNA-binding activity of HetR appear to block heterocyst development at an early stage (Risser and Callahan, 2007).

There is evidence that the pattern formed during heterocyst development conforms to the activator-inhibitor model as it is described by Grierer and Meinhardt (Grierer and Meinhardt, 1972). In the case of *Anabaena*, it is thought that the activator is HetR and that there are two inhibitors, PatS and HetN. Both PatS and HetN suppress heterocyst development, and HetR promotes their development. PatS has been shown to be involved in the establishment of the *de novo* pattern; *patS* mutants initially form a pattern of multiple contiguous heterocysts (Mch) that resolve to a normal pattern (single heterocysts approximately every tenth cell) by 72 hours after nitrogen starvation (Yoon and Golden, 2001). The PatS pentapeptide RGSGR has been shown to be sufficient to repress heterocyst development when expressed ectopically (Yoon and Golden, 1998). HetN plays a role in the maintenance of the pattern as the filament continues to grow and divide. A mutation in this gene leads to a Mch phenotype after 48 hours (Callahan and Buikema, 2001). It is believed that the mode of action of the inhibitors, PatS and HetN, is inactivation of HetR after diffusion along the filament (Risser and Callahan, 2009).

The Act of Commitment of Heterocyst Cells

The act of commitment, which lies between the more understood processes of pattern formation and morphogenesis of mature heterocysts, in the heterocyst developmental pathway, is one of the major gaps in the current model of heterocyst development. Commitment of cells destined to differentiate into heterocysts occurs

between 9 and 14 hours after nitrogen deprivation. Prior to this time, the process of differentiation is reversible if a supply of fixed nitrogen is restored to the culture (Thiel and Pratte 2001; Yoon and Golden 2001). Due to the fact that heterocyst cells do not proliferate, it is reasonable to assume that commitment to differentiation is highly regulated. Genes identified as being associated with heterocyst development that act downstream of *hetR* and are not linked directly to heterocyst morphogenesis are considered candidates for key players in the process of heterocyst commitment.

Mature Heterocyst Cells are Capable of Fixing Atmospheric Nitrogen

Maturation of heterocyst cells occurs down-stream of initiation, patterning, and commitment in the heterocyst developmental pathway (Figure 2). A mature heterocyst cell is a terminally differentiated cell, specific to fixing atmospheric nitrogen by production of oxygen-labile nitrogenase. To create a microoxic environment, heterocyst cells deposit a glycolipid layer that acts as a physical barrier to oxygen and a layer of exopolysaccharide that is thought to protect the glycolipid. Additionally, increased intracellular respiration rates lower cytoplasmic oxygen levels while photosystem II and its associated phycobilliproteins are inactivated to prevent the evolution of oxygen as a byproduct of photosynthesis. A loss of the phycobilliproteins is visualized on a micrograph as the loss of UV-excited auto-fluorescence emitted in the red region of the visible spectrum. Only after a microoxic environment is established in the heterocyst cell does nitrogenase fix environmental di-nitrogen into ammonia that is then transported to neighboring vegetative cells in the form of glutamate and glutamine.

HetP Plays a Role in Heterocyst Differentiation

The gene *hetP* was originally identified in a transposon-mutant screen and found to be required for heterocyst differentiation. Initially, the *hetP* mutant was characterized as incapable of forming heterocyst cells; however, upon further investigation it was determined that the mutant strain eventually forms heterocyst cells, albeit delayed by 48 to 72 hours (Fernandez-Pinas, et al, 1994). During the investigation of the *hetP* transposon mutant, it was determined that the presence of *hetP* on a multi-copy plasmid was capable of complementing the transposon mutant. In a wild-type strain, the presence of a similar plasmid resulted in the formation of multiple contiguous heterocysts (Mch) (Higa and Callahan, 2010).

Deletion of *hetP* from the chromosome yielded a phenotype similar to that previously described for the *hetP* transposon mutant strain. Namely, the mutant did not form heterocysts at 24 hours after nitrogen starvation but did form a reduced number (1-2%) at 48 hours. Acetylene reduction assays demonstrated that the heterocyst cells produced in the mutant strain were mature and capable of fixing nitrogen (Higa and Callahan, 2010).

Recent research has indicated that *hetP* functions directly downstream of HetR in the regulatory network responsible for heterocyst differentiation. Ectopic expression of *hetP* from an inducible promoter in a Δ*hetR* mutant strain leads to the development of cells morphologically similar to heterocyst cells. However, nitrogenase activity of these cells is only detected under anaerobic conditions (Higa and Callahan, 2010). This is significant because HetR had been considered both absolutely necessary and sufficient for heterocyst differentiation and was thus referred to as the “master regulator of

heterocysts." An inverted repeat sequence in the promoter region of *hetP* was shown to bind HetR as demonstrated through electrophoretic mobility shift assays (EMSA) (Higa, 2010). Promoter fusions of the native *hetP* promoter to GFP in a Δ*hetR* background also suggest that the HetR protein is involved in regulating the transcription of *hetP*, either directly or indirectly (Higa, 2010). Transcription of *hetR* and *patS*, two known genes involved in patterning, appear normal when viewed with a GFP reporter in the *hetP* mutant strain (Higa and Callahan 2010). This data suggests that *hetP* is working down-stream of HetR in the heterocyst developmental pathway.

Taken together, there are three lines of evidence that suggest *hetP* may be involved in the commitment of heterocyst development: 1) HetP is required for normal heterocyst differentiation and appears to act downstream of *hetR* transcription; 2) HetP is not required for expression of patterning genes as they appear to be normal in a *hetP* mutant; and 3) there is no data that suggests that *hetP* is directly involved in heterocyst maturation. Additionally, expression of *hetP* increases 2.5-fold six hours after removal of nitrogen (Fernandez-Pinas, et al. 1994). Since commitment occurs sometime between 9 and 14 hours, the expression of *hetP* falls within a reasonable time period to function in heterocyst commitment.

The exact function of HetP is unknown and BLAST (Basic Local Alignment Search Tool) analysis of HetP did not reveal any similarities to known protein sequences; however, three homologous genes were identified in the *Anabaena* genome. The three genes homologous to *hetP* were identified as: *asl1930, alr2902,* and *alr3234* (Higa and Callahan, 2010). The homologues will be referred to as *hetP1*, *hetP2*, and *hetP3* as outlined in Table 1, below. Alignment of HetP along with the predicted amino acid

sequences of the three homologues revealed that the level of highest sequence similarity corresponds to amino acids 13-63 of HetP (Figure 3).

Table 1: *hetP* homologues and their corresponding codes

asl1930	*hetP1*
alr2902	*hetP2*
alr3234	*hetP3*

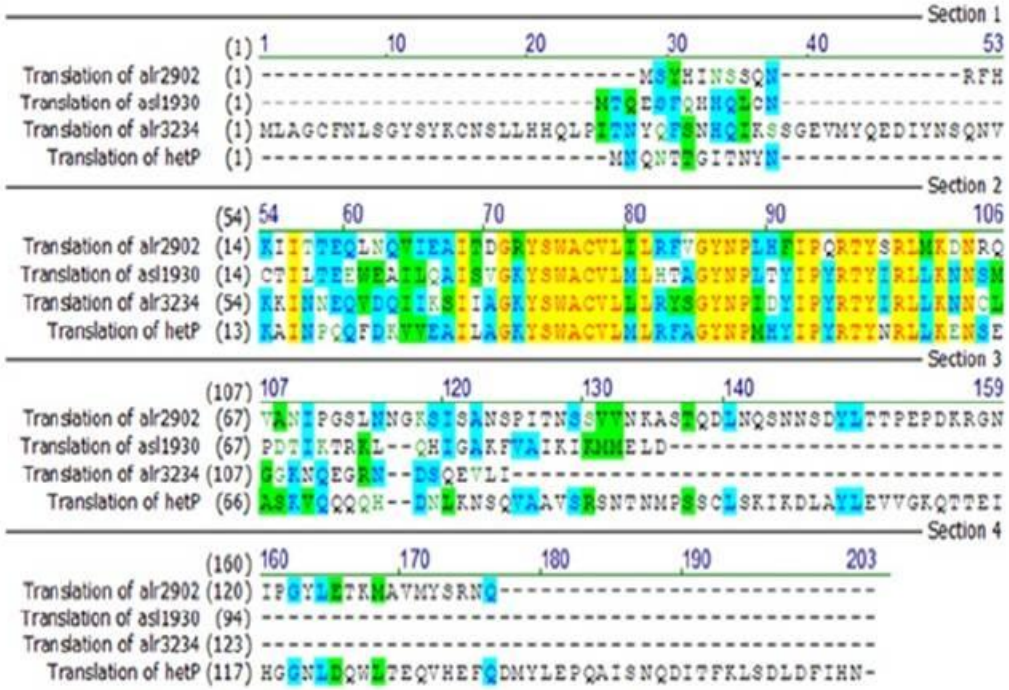

Figure 3: Amino acid alignment of the proteins encoded by *hetP*, *alr2902*, *alr3234*, and *asl1930* (Higa and Callahan, 2010).

Possible functional redundancy of the *hetP* homologues was investigated by placing each of the homologues under the control of the *petE* promoter on multi-copy shuttle vectors and individually introducing them into the Δ*hetP* strain (Higa and Callahan, 2010). Overexpression of each of the homologues in the Δ*hetP* background resulted in slightly different phenotypes, suggesting their functions may be dissimilar.

No complementation was seen when *hetP1* was overexpressed in the Δ*hetP* strain. This construct resulted in heterocyst percentages similar those of the Δ*hetP* strain alone at 72 hours after nitrogen starvation. Conversely, the overexpression of *hetP2* produced wild-type percentages of heterocysts by 48 hours after the removal of fixed nitrogen in the Δ*hetP* strain. The overexpression of *hetP3* displayed a Δ*hetP* phenotype at 48 hours after nitrogen removal; however, by 72 hours the phenotype appeared wild type (10% heterocysts). In comparison, the overexpression of *hetP* in a Δ*hetP* strain yields a wild-type phenotype after 48hrs of nitrogen starvation. Therefore, it was determined that the overexpression of both *hetP2* and *hetP3* can functionally complement a Δ*hetP* mutant. Unlike the overexpression of *hetP* in the Δ*hetR* background, none of the *hetP* homologues were capable restoring formation of heterocysts to a Δ*hetR* mutant.

CHAPTER 2. MATERIALS AND METHODS

Bacterial Strains and Growth Conditions

Escherichia coli strains and derivatives were grown in Terrific broth (TB) for liquid overnight cultures, Luria-Bertani (LB) broth for conjugation liquid cultures, and LB plates for plated cultures. To select for *E. coli* carrying plasmids, media was supplemented with ampicillin (Ap) at 100 μg/ml or 50 μg/ml when in combination with other antibiotics, kanamycin (Km) at 50 μg/ml, spectinomycin (Sp) at 100 μg/ml, or chloramphenicol (Cm) at 10 μg/ml. Cultures were grown at 37°C.

Anabaena sp. PCC 7120 and its derivatives were grown in BG-11 medium as previously described (Buikema and Haselkorn 1991). Plates were supplemented with 1 μg/ml of carbendizim and 1 mM $Na_2S_2O_3$. Liquid cultures were supplemented with 10 mM HEPES and 5 mM $NaHCO_3$. When selecting for plasmids, media was supplemented with spectinomycin (Sp) and streptomycin (Sm) at 2.5 μg/ml each or neomycin (Nm) at 45 μg/ml. Induction of heterocysts was performed as previously described (Borthakur, Orozco et al. 2005). Cultures were grown in an incubator at 30°C with continuous light and 2% CO_2.

Conjugal transfer of plasmids from *E. coli* to *Anabaena* sp. PCC 7120 and its derivatives was done as previously described (Elhai and Wolk 1988).

Plasmid Construction

Plasmids pPJAV232, pPJAV233, pPJAV234, pPJAV235, pPJAV236, pPJAV237, and pPJAV244 were used to create strains with an allele of *hetP* lacking a range of amino acids: Δ26-159, Δ51-159, Δ68-159, Δ75-159, Δ100-159, Δ125-159, and native length *hetP*, respectively. The fragments used to make truncations were amplified via overlap

extension PCR (Higuchi *et al.*, 1988) using chromosomal DNA as a template. The primers used to create the downstream fragment were hetP-down-EcoRV-F and hetP-down-SmaI-R. The following primers were used to make specific *hetP* alleles: hetP-up-XhoI and hetP-25aa-EcoRV-R for pPJAV232; hetP-up-XhoI and hetP-50aa-EcoRV-R for pPJAV233; hetP-up-XhoI and hetP-68aa-EcoRV-R for pPJAV234; hetP-up-XhoI and hetP-75aa-EcoRV-R for pPJAV235; hetP-up-XhoI and hetP-100aa-EcoRV-R for pPJAV236; hetP-up-XhoI and hetP-125aa-EcoRV-R for pPJAV237; and hetP-up-XhoI and hetP-159aa-EcoRV-R for pPJAV244. The overlap extension PCR products were cloned into the SmaI site in pBlueScript SK+. These were all excised as SalI-SpeI fragments and cloned into the XbaI-XhoI sites in pRL277.

Plasmids pPJAV238, pPJAV239, and pPJAV240 were used to reintroduce *hetP* alleles encoding C36A, C95A, and C36A/C95A substitutions, respectively, into *Anabaena*, effectively replacing the *hetP* locus of PCC 7120. The fragments used to make base substitutions were amplified via overlap extension PCR (Higuchi *et al.*, 1988) using chromosomal DNA as a template. The outer primers used to create the constructs were hetP-up-XhoI and hetP-down-SmaI-R. The following primers were used to create specific *hetP* alleles: hetPC36A-F M475L and hetPC36A-R M475L for pPJAV238; hetPC95A-F M475L and hetPC95A-R M475L for pPJAV239; and, using pPJAV238 as a template, hetPC95A-F M475L and hetPC95A-R M475L for pPJAV240. The overlap extension PCR products were cloned into the SmaI site in pBlueScript SK+. These were all excised as SalI-SpeI fragments and cloned into the XbaI-XhoI sites in pRL277.

The plasmids pPJAV298, pPJAV299, pPJAV300, pPJAV301, pPJAV302, pPJAV303, and pPJAV304 are mobilizable shuttle vectors based on pAM504 carrying

alleles of *hetP* lacking a range of amino acids: Δ26-159, Δ51-159, Δ69-159, Δ76-159, Δ101-159, Δ126-159, and native length *hetP*, respectively, transcriptionally fused to the native *hetP* promoter. These fragments were amplified via PCR using chromosomal DNA as a template. The upstream primer used to create these fragments was hetP-up-XhoI, and the following downstream primers were used to make specific *hetP* alleles: hetP-25aa-EcoRV-R for pPJAV298; hetP-50aa-EcoRV-R for pPJAV299; hetP-68aa-EcoRV-R for pPJAV300; hetP-75aa-EcoRV-R for pPJAV301; hetP-100aa-EcoRV-R for pPJAV302; hetP-125aa-EcoRV-R for pPJAV303; and hetP-159aa-EcoRV-R for pPJAV304. These were cloned as XhoI-EcoRV fragments and cloned into the SalI-SmaI sites in pAM504.

Plasmids pPJAV305, pPJAV306, and pPJAV307 are mobilizable shuttle vectors based on pAM504 carrying alleles of *hetP* encoding C36A, C95A, and C36A/C95A substitutions, respectively, driven by the native *hetP* promoter. The fragments used to make base substitutions were amplified via overlap extension PCR (Higuchi *et al.*, 1988) using chromosomal DNA as a template. The outer primers used to create the constructs were hetP-up-XhoI and hetP-159aa-EcoRV-R. The following primers were used to create specific *hetP* alleles: hetPC36A-F M475L and hetPC36A-R M475L for pPJAV305; hetPC95A-F M475L and hetPC95A-R M475L for pPJAV306; and, using pPJAV238 as a template, hetPC95A-F M475L and hetPC95A-R M475L for pPJAV307. These were cloned as XhoI-EcoRV fragments and cloned into the SalI-SmaI sites in pAM504.

Plasmid pPJAV295 is a mobilizable shuttle vector based on pAM504 containing the gene for the flavin mononucleotide-based fluorescent protein (FbFP), *FbFP*, transcriptionally fused to the *nifB* promoter. The coding region of *FbFP* was excised

from pGLOW-Kxn-Bs1 as a BamHI-XbaI fragment, blunt-ended with T4 DNA polymerase, cloned into the SmaI site of pBlueScript SK+, and screened for directionality by PCR (co-linear with the *lac* promoter) creating pPJAV216. The coding region of *FbFP* was PCR amplified from pPJAV216 with the primers M13R and FbFP-BglII-R. The product was digested with BamHI-BglII and cloned into the BamHI sites of pAM1956 creating pPJAV222. The *nifB* promoter was amplified by PCR from PCC 7120 chromosomal DNA with the primers PnifB-XhoI-F and PnifB-EcoRV-R. The product was digested with EcoRV, cloned into the SmaI site of pPJAV22, and screened for directionality with PCR creating pPJAV295.

Plasmid pKH239 is a suicide vector used to cleanly delete the nucleotides of *alr2902* starting at nucleotide 11 and continuing 97 nucleotides past the stop codon of the 498 base pair coding region. Chromosomal DNA upstream of the *alr2902* coding region was amplified via PCR using primers d2902-up-F and d2902-up-R. Chromosomal DNA downstream of the *alr2902* coding region was amplified via PCR using primers d2902-dn-F and d2902-dn-R. These PCR products were used in overlap extension PCR and amplified with primers d2902-up-F and d2902-dn-R. The product was cloned into pRL277 as a *Bgl*II-*Sac*I fragment to create pKH239.

Plasmid pKH241 is a suicide vector used to cleanly delete nucleotides 18-264 of the 282 base-pair coding region of *alr3234*. Chromosomal DNA upstream of the *alr3234* coding region was amplified via PCR using primers d3234-up-F and d3234-up-R. Chromosomal DNA downstream of the *alr3234* coding region was amplified via PCR using primers d3234-dn-F and d3234-dn-R. These PCR products were used in overlap extension PCR and amplified with primers d3234-up-F and d3234-dn-R. The product

was cloned into pRL277 as a *Bgl*II-*Sac*I fragment to create pKH241.

Plasmid pKH242 is a suicide vector used to replace the *alr3234* coding region with a spectinomycin/streptomycin resistance cassette. Chromosomal DNA upstream of the *alr3234* coding region was amplified via PCR using primers d3234-up-F and d3234-up-R. Chromosomal DNA downstream of the *alr3234* coding region was amplified via PCR using primers d3234-dn-F and d3234-dn-R. These PCR products were used in overlap extension PCR and amplified with primers d3234-up-F and d3234-dn-R. The amplification product was cloned into the SmaI site of pBlueScript SK+, digested with SmaI, and the spectinomycin/streptomycin resistance cassette from pDW9 was cloned in as a SmaI fragment. The entire fragment was cloned into pRL278 the *BamH*I-*Sac*I sites as a *Bgl*II-*Sac*I fragment to create pKH242.

Plasmid pKH274 is a suicide vector used to cleanly delete nucleotides 15-359 of the 369 base-pair coding region of *asl1930*. Chromosomal DNA upstream of the *asl1930* coding region was amplified via PCR using primers 1930-up-F and 1930-up-R. Chromosomal DNA downstream of the *asl1930* coding region was amplified via PCR using primers 1930-dn-F and 1930-dn-R. These PCR products were used in overlap extension PCR and amplified with primers 1930-up-F and 1930-dn-R. The product was cloned into pRL277 as a *Bgl*II-*Sac*I fragment to create pKH274.

Plasmid pPJAV123 is a mobilizable shuttle vector based on pAM504, in which the *Nde*I site was removed by digestion with *Nde*I and blunt-ending with T4 DNA polymerase followed by ligation. pPJAV153 is a mobilizable shuttle vector based on pAM504 used to make C-terminal translational protein fusions to yellow fluorescent protein (YFP), *YFP*, transcriptionally driven by the *petE* promoter. The coding region of

YFP was amplified by PCR using pUC57-P_{S12}-YFP (Norris *et al*., 2010) as a template with primers PpetE-Cterm-OEX-F and TurboYFP-CtermR-SacI. The *petE* promoter was amplified using PCC 7120 chromosomal DNA as a template with primers PpetE-XhoI-F and PpetE-Cterm-OEX-R. These PCR products were used in overlap extension PCR and amplified with primers PpetE-XhoI-F and TurboYFP-CtermR-SacI. The resulting product was cloned into the *Sma*I site of pBlueScript SK+. The *Xho*I-*Sac*I fragment containing PpetE-YFP was cloned into the *Sal*I-*Sac*I sites of pPJAV123 to create pPJAV153.

Plasmid pLMC115 is a mobilizable shuttle vector based on pAM504 containing the yellow fluorescent protein (YFP) translationally fused to the C-terminus of the *ftsZ* open reading frame and under the control of the *petE* promoter. The coding region of *ftsZ* was PCR amplified from PCC 7120 chromosomal DNA with the primers PpetE-FtsZ-YFP/CFP F (NdeI) and PpetE-FtsZ-YFP/CFP R (BamHI) and cloned into the NdeI/BamHI site of pPJAV153 to make pLMC115.

Plasmid pKLH101 is a mobilizable shuttle vector containing $P_{alr3234}$-gfp. A region 886 base pairs up-stream of *alr3234*, into the *trpE* coding region, was amplified from chromosomal DNA with the primers F-alr3234-pro-into trpE and R-alr3234-pro-into trpE and cloned into EcoRV of pBlueScriptSK+. The fragment containing the promoter region was cut out as a KpnI/SacI fragment and cloned into pAM1956.

Plasmid pKLH103 is a mobilizable shuttle vector containing $P_{asl1930}$-gfp. A region 650 base pairs up-stream of asl1930, into the gene all 1931, was amplified from chromosomal DNA with primers F-pro-asl1930 into all1931and R-asl1930 promoter region primer. The DNA fragment was cloned into EcoRV of pBlueScriptSK+ and cut

out as a KpnI/SacI fragment and cloned into pAM1956.

Plasmid pKLH104 is a mobilizable shuttle vector containing $P_{alr2902}$-gfp. A region 638 base pairs up-stream of alr2902 was amplified from chromosomal DNA with primers fwd-alr2902-promoter-region and R-alr2902 promoter primer. The DNA fragment was cloned into EcoRV of pBlueScriptSK+ and cut out as a KpnI/SacI fragment and cloned into pAM1956.

All plasmids were sequenced with appropriate sequencing primers pRLs-Sac, pRL277-BglII, pRL278-BamHI, 505-Bam, 505-Sac, M13-F, M13-R, PpetE-int-F, or turbo-int-R to verify their integrity.

Strain Construction

***hetP* and *hetP*-homologue deletions.** Clean deletion of chromosomal DNA was performed as previously described (Callahan and Buikema 2001) with the following combinations of strains and plasmids: 7120 and pKH239 for construction of Δ*hetP2*; ; 7120 and pKH274 for Δ*hetP1*; Δ*hetP* and pKH239 for Δ*hetP*Δ*hetP2*; ΔhetP and pKH241 for construction of Δ*hetP*Δ*hetP3*; Δ*hetP* and pKH274 for construction of Δ*hetP*Δ*hetP1*; Δ*hetP*Δ*hetP1* and pKH239 for Δ*hetP*Δ*hetP1*Δ*hetP*2; Δ*hetP*Δ*hetP1* and pKH241 for construction of Δ*hetP*Δ*hetP1*Δ*hetP*3; Δ*hetP*Δ*hetP2* and pKH241 for construction of Δ*hetP*Δ*hetP2*Δ*hetP*3; Δ*hetP1* and pKH239 for construction of Δ*hetP1*Δ*hetP2*. Clean deletions were confirmed by amplifying DNA from strains using primers flanking the region used for recombination on pKH239, pKH241, and pKH274: del-2902-up-out and del-2902-dn-out; del-3234-up-out and del-3234-dn-out; del-1930-up-out and del-1930-dn-out, respectively.

Δ*hetP*Δ*hetP1*Δ*hetP*2 Δ*hetP*$3_{sp/sm}$, was constructed using pKH242, which contains a spectinomyocin/streptomycin cassette, into the previously constructed strain Δ*hetP*Δ*hetP1*Δ*hetP*2. The strain was verified by PCR using the primers del-3234-up-out and del-3234-dn-out.

Truncated forms of HetP. Chromosomal replacements of the *hetP* gene with alleles encoding one of the six truncated forms of HetP (25, 50, 68, 75, 100, or 125 N-terminal fragments) were made by introducing suicide vectors containing the various truncations into a Δ*hetP* strain. The six truncated versions of *hetP* were introduced to the chromosome with the following strain and plasmid combinations: Δ*hetP* and pPJAV232 for construction of *HetPΔ26-159*; Δ*hetP* and pPJAV233 for construction of *HetPΔ51-159*; Δ*hetP* and pPJAV234 for construction of *hetPΔ69-159*; Δ*hetP* and pPJAV235 for construction of h*etPΔ76-159*; Δ*hetP* and pPJAV236 for construction of h*etPΔ101-159*; Δ*hetP* and pPJAV237 for construction of h*etPΔ126-159*; and Δ*hetP* and pPJAV244 was used to reintroduce the full-length version of *hetP* to the chromosome. The resulting truncation strains were confirmed by amplifying DNA from strains using the primers del-hetP-up-out and del-hetP-dn-out.

Cysteine mutations in HetP. Strains containing *hetP* with substitution of the cysteine codons (amino acids 36 and 95) with those encoding alanine residues individually and in combination were constructed. The following plasmids were introduced into a Δ*hetP* strain to create the mutants *hetPc36A*, *hetPc95A*, and h*etPc36/95A*, respectively: pPJAV305, pPJAV306, and pPJAV307. These strains were maintained as single-recombinants on BG11 plates supplemented with 2.5 μg/mL of Sp/Sm.

Heterocyst Counts and Microscopy

Cells were viewed with a light microscope as previously described (Borthakur, et al. 2005). Heterocyst counts were done by counting 500 cells and recording the number of heterocysts. Fluorescence pictures were taken at an exposure 10-20 milliseconds for red autofluorescence, 1 second for GFP (green fluorescent protein) and 500 milliseconds for YFP (yellow fluorescent protein) and CFP (cyan fluorescent protein). Cells were viewed with a confocal microscope as previously described (Higa, 2012). FbFP and CFP fluorescence were detected with excitations of 450nm and 405nm and emissions of 470nm and 458nm, respectively on an Olympus Fluoview confocal.

Acetylene Reduction and Exopolysaccharide Assays

Aerobic and anaerobic acetylene reduction assays were performed as previously described (Ernst, et al. 1992, Borthakur, et al. 2005).

Heterocyst envelope polysaccharide was stained with 0.5% Alcian blue made in a 50% ethanol solution by mixing 2.5 µl of culture and 2.5 µl of stain and visualizing 2 µl of the mixture on a slide.

Table 2: Plasmids used in this study.

Plasmid	Relevant characteristic(s)	Source or Reference
pAM504	Mobilizable shuttle vector for replication in *E. coli* and *Anabaena*; Km^rNeo^r	(Wei, Ramasubramanian et al. 1994)
pAM505	Same as pAM504 with multiple cloning site inverted	(Wei, Ramasubramanian et al. 1994)
pAM1956	Mobilizable shuttle vector based on pAM505 carrying *gfp*; used to make *gfp* transcriptional fusions	(Yoon and Golden 1998)
pAM1951	Mobilizable shuttle vector based on pAM504 carrying p*Pats-gfp*	(Yoon and Golden 1998)
pGLOW-Kxn-Bs1	Source of FbFP	(Evocatal)
pDR110	pBluescript::P_{petE}	This study
pRL277	Suicide vector; Sm^rSp^r	(Black, Cai et al. 1993)
pRL278	Suicide vector; Km^r/Nm^r	(Black, Cai et al. 1993)
pDW9	Plasmid carrying the Sm^rSp^r cassette	(Golden and Wiest 1988)
pKH239	Suicide vector based on pRL277 used to delete *hetP2 (alr2902)*	This study
pKH241	Suicide vector based on pRL277 used to delete *hetP3 (alr3234)*	This study
pKH242	Suicide vector based on pRL277 used insert sp/sm in hetP3 (*alr3234)*	This study
pKH274	Suicide vector based on pRL277 used to delete *hetP1 (asl1930)*	This study
pKLH101	pAM504 carrying P*alr3234-gfp*	This study
pKLH103	pAM504 carrying P*alr1930-gfp*	This study
pKLH104	pAM504 carrying P*alr2902-gfp*	This study
pLMC115	pAM504 carrying P_{hetP}-*ftsZ*-y*fp*	This study
pPJAV123	pAM504 with NdeI site removed	This study
pPJAV153	Mobilizable shuttle vector based on pAM504 carrying P*petE* used to translationally fuse YFP to create C-terminal translational fusions	This study
pPJAV216	FbFP in pBSK+	This study
pPJAV222	Promoterless FbFP	This study
pPJAV232	Suicide vector based on pRL277 used to replace *hetP* with *hetP*(25aa)	This study
pPJAV233	Suicide vector based on pRL277 used to replace *hetP* with *hetP*(50aa)	This study
pPJAV234	Suicide vector based on pRL277 used to replace *hetP* with *hetP*(68aa)	This study
pPJAV235	Suicide vector based on pRL277 used to replace *hetP* with *hetP*(75aa)	This study
pPJAV236	Suicide vector based on pRL277 used to replace *hetP* with *hetP*(100aa)	This study
pPJAV237	Suicide vector based on pRL277 used to replace *hetP* with *hetP*(125aa)	This study
pPJAV238	Suicide vector based on pRL277 used to replace *hetP* with *hetP*(C36A)	This study
pPJAV239	Suicide vector based on pRL277 used to replace *hetP* with *hetP*(C95A)	This study
pPJAV240	Suicide vector based on pRL277 used to replace *hetP* with	This study

	hetP(C36/95A)	
pPJAV244	Suicide vector based on pRL277 used to replace *hetP* with *hetP*	This study
pPJAV295	pAM504 carrying P_{nifB}-FbFP	This study
pPJAV298	pAM504 carrying p*hetP hetP*(25aa)	This study
pPJAV299	pAM504 carrying p*hetPhetP*(50aa)	This study
pPJAV300	pAM504 carrying p*hetPhetP*(68aa)	This study
pPJAV301	pAM504 carrying p*hetPhetP*(75aa)	This study
pPJAV302	pAM504 carrying p*hetPhetP*(100aa)	This study
pPJAV303	pAM504 carrying *phetPhetP*(125aa)	This study
pPJAV304	pAM504 carrying *phetPhetP*(25)	This study
pPJAV305	pAM504 carrying *phetPhetP*(C36A)	This study
pPJAV306	pAM504 carrying *phetPhetP*(C95A)	This study
pPJAV307	pAM504 carrying *phetPhetP*(C3/95A)	This study
pSMC232	Mobilizable shuttle vector based on pAM505 carrying *gfp*; used to make *gfp* translational fusions	This study
pUC57-PS12-yfp	pUC plasmid containing YFP turbo	(Norris *et al*., 2010)

Table 3: Bacterial strains used in this study.

Strain	Relevant characteristic(s)	Source or reference (UHM designation)
Anabaena sp. strain PCC 7120	Wild-type	Pasteur Culture Collection
Δ*hetR*	*hetR*-deletion strain	(Borthakur, Orozco et al. 2005) UHM103
Δ*hetP*	*hetP*-deletion strain	(Higa, 2010) UHM158
Δ*hetP*Δ*hetP1*	*hetP*-, *asl1930*- deletion strain	This Study UHM 288
Δ*hetP*Δ*hetP2*	*hetP*-, *alr2902*- deletion strain	This Study UHM 287
Δ*hetP*Δ*hetP3*	*hetP*-, *alr3234*- deletion strain	This Study UHM 286
Δ*hetP*Δ*hetP1*Δ*hetP2*	*hetP*-, *asl1930*-, *alr2902*-deletion strain	This Study UHM 282
Δ*hetP*Δ*hetP1*Δ*hetP3*	*hetP*-, *asl1930*-, *alr3234*-deletion strain	This study UHM 283
Δ*hetP*Δ*hetP2*Δ*hetP3*	*hetP*-, *alr2902*-, *alr3234*-deletion strain	This study UHM 284
Δ*hetP*Δ*hetP1* Δ*hetP2*Δ*hetP3*$_{sp/sm}$	*hetP*-, *asl1930*-, *alr2902*-deletion strain, *alr3234* sp/sm cassette insertion	This study UHM 285
Δ*hetP1*	*asl1930*- deletion strain	This study UHM 295
Δ*hetP2*	*alr2902*- deletion strain	This study UHM 296
Δ*hetP3*	*alr3234*-deletion strain	This study UHM
HetPΔ26-159	HetP-25 amino acid truncation mutant	This study UHM 294
HetPΔ51-159	HetP-50 amino acid truncation mutant	This study UHM 293
HetPΔ69-159	HetP-68 amino acid truncation mutant	This study UHM 292
HetPΔ76-159	HetP-75 amino acid truncation mutant	This study UHM 291
HetPΔ101-159	HetP-100 amino acid truncation mutant	This study UHM 290
HetPΔ126-159	HetP-125 amino acid truncation mutant	This study UHM 289
HetPc36A	HetP C→A mutation at amino acid 36	This study Single Recomb
HetPc95A	HetP C→A mutation at amino acid 95	This study Single Recomb.

Table 4: Oligonucleotides used in this study.

Oligonucleotide	Sequence in 5' to 3' direction
pRLs-Sac	TGTAGATAACTACGATACGG
pRL277-BglII	TAAGGCAGTTATTGGTGC
pRL278-BamHI	TTCTATGAAAGGTTGGGCTTCG
505-Bam	CTACGGGGTCTGACGCTCAGTGG
505-Sac	GTCGAACTGCGCGCTAACTATTC
M13-F	GTAAAACGACGGCCAGTG
M13-R	GGAAACAGCTATGACCATG
d2902-up-F	ATATAAGATCTAGTGATTCTTCATCTCCCTC
d2902-up-R	TTTTCCGATACCCGGGTAGCTCATAGTGTCTTGGAG
d2902-dn-F	CTATGAGCTACCCGGGTATCGGAAAAAGCTAGGTTC
d2902-dn-R	ATATAGAGCTCATAACTGTCCTAGAGATAGC
2902-up-out	ATCTGTCTTTGCTACGCAAC
2902-dn-out	TCCAATAACTTACCCACGAC
Fwd-alr2902-promoter region	TTTGAGCTCGGACGTAGGAAAATTGTATTCTG
R-alr2902 promoter primer	TTTGGTACCAGTGTCTTGGAGATATTTATCTA AATATGAAATTTATAG
d3234-up-F	ATATAAGATCTAACTCAAGGAAACGATAGTC
d3234-up-R	TCAAATCAAGCCCGGGCATCCAGCTAACATCAAACC
d3234-dn-F	TAGCTGGATGCCCGGGCTTGATTTGAACCACATCTG
d3234-dn-R	ATATAGAGCTCTTTCGATTAAGCGAACATCG
3234-up-out	ACAATTACTAAAGCGACTGC
3234-dn-out	ATAAGTTTTGGGTGGTACTG
F-alr3234-pro-into trpE	TTTGAGCTCATTCGTTTACAAGACTCCATCGC CG
R-alr3234-pro-into trpE	TTTGGTACCCAAACCCTGATAAAACAAGACTT TCAATCTG
1930-up-F	ATATAAGATCTATCGGGATGGTTTAACTCTC
1930-up-R	TTCCATCATCCCGGGAAAGATTCTTGAGTCATCAGC
1930-dn-F	CAAGAATCTTTCCCGGGATGATGGAATTAGATTAAAG
1930-dn-R	ATATAGAGCTCAAGAACTACAACAATCTGC
1930-up-out	GAAGAATCAGATGGGACTTTGGC
1930-dn-out	CCCAGAAAATCATTGCTGATACTCCTG
F-pro-asl1930 into all1931	TTTGAGCTCTATCAAACTTTGGTACGTGTTTA ACTCCAG
R-asl1930 promoter region primer	TTTGGTACCATATTTAAGATGAGTTACAACAT TTATATCTAAATATTTGTAG
hetP-down-EcoRV-F	GATATCTGATGTGACTTCGGGGTTGTGTATC
hetP-down-SmaI-R	ATATATCCCGGGCCATGATGGATTAGTTCATAGTGTTG
hetP-up-XhoI	ATATACTCGAGTTGTCTAGTCAGTTGTCAGTCGTCAATAG
hetP-25aa-EcoRV-R	GAAGTCACATCAGATATCTCATTCAACCACTTTGTCAAATTGTTGAGGATTG
hetP-50aa-EcoRV-R	GAAGTCACATCAGATATCTCAGTAGTGCATAGGATTGTACCCAGCAAAGCG

hetP-68aa-EcoRV-R	GAAGTCACATCAGATATCTCATTTGCTAGCTTCGGAGTTTTCTTTGAG
hetP-75aa-EcoRV-R	GAAGTCACATCAGATATCTCAATCGTGTTGTTGTTGCTGTACTTTGC
hetP-100aa-EcoRV-R	GAAGTCACATCAGATATCTCAGATTTTACTTAAGCAACTGGACGGC
hetP-125aa-EcoRV-R	GAAGTCACATCAGATATCTCATAACCATTGATCTAAATTACCACCATG
hetP-159aa-EcoRV-R	GAAGTCACATCAGATATCTCAATTATGAATAAAATCTAGGTCTGACAGTTTG
hetPC36A-F M475L	AAATACTCTTGGGCTGCTGTTCTCATGCTGCG
hetPC36A-R M475L	CGCAGCATGAGAACAGCAGCCCAAGAGTCTTT
hetPC95A-F M475L	AATATGCCGTCCAGTGCCTTAAGTAAAATCAA
hetPC95A-R M475L	TTGATTTTACTTAAGGCACTGGACGGCATATT
FbFP-BglII-R	TATATAGATCTTTACATAATCGGAAGCACTTTAACG
PnifB-XhoI-F	ATATACTCGAGAGCAACTGCGTCTGATAGTGTTAATAATGGCTTGG
PnifB-EcoRV-R	ATATAGATATCTCAGTAACGGAAGAGCCTGTAACTGGTGGTG
PpetE-Cterm-OEX-F	GAGCTCTCAGCTGGTGTCTCCGGAACCGG
TurboYFP-CtermR-SacI	GAGCTCTCAGCTGGTGTCTCCGGAACCGG
Turbo-int-R	CATCTCCACCACGTAGGGGATCTTG
PpetE-int-F	CGAAGTATGACAGATTGTCATATTTGGTGTC
PpetE-XhoI-F	TATATCTCGAGGCTGAGGTACTGAGTACACAGC
PpetE-FtsZ-YFP/CFP F (NdeI)	AGGAGAGGAGCATATGACACTTGATAATAACCAAGAGCTTAC
PpetE-FtsZ-YFP/CFP R (BamHI)	CTCCTGGATCCATTTTTGGGTGGTCGCCGTCTCT

CHAPTER 3. REGIONS OF HETP NECESSARY FOR FUNCTION

The Minimum Length of HetP that Retains Function

The HetP protein is comprised of 159 amino acids. To determine the minimum functional length of HetP, genes encoding truncated forms of HetP were created. Six total *hetP* truncations were made, each driven by the native *hetP* promoter, and corresponded to the first 25, 50, 68, 75, 100, or 125 amino acids of the HetP protein. The truncations were introduced on mobilizable shuttle vectors (pPJAV298-pPJAV303) into wild-type, Δ*hetP*, and Δ*hetR*, backgrounds, and the resulting strains were observed to determine their ability to differentiate heterocysts.

Overexpression of *hetP*, from the *petE* promoter on a multi-copy plasmid in a wild-type strain typically causes differentiation of a greater percentage of heterocyst cells than the wild-type strain not carrying the plasmid (Higa, 2010). None of the truncated genes promoted greater than wild-type percentages of heterocysts when expressed behind the native promoter of *hetP* in a wild-type strain (data not shown). However, heterocyst cells were occasionally observed in the wild-type strains containing the truncated genes coding the 68, 75, 100, or 125 amino acid fragments when observed directly from plates containing ammonia; media which typically suppresses differentiation. When grown without a source of fixed nitrogen the truncation strains differentiated heterocysts, but never in percentages greater than wild type.

The *hetP*-truncation plasmids under the control of the native *hetP* promoter were not capable of bypassing the need for *hetR*. This is not surprising because a plasmid carrying a full-length version of *hetP* driven by its native promoter also failed to produce heterocysts in a Δ*hetR* background. This suggests that a specific threshold of HetP must

be surpassed in order for HetP to bypass the need for HetR during the differentiation process.

Complementation of a Δ*hetP* mutant was attempted by introduction of the various *hetP* truncations on plasmids. Since a Δ*hetP* mutant is capable of producing a small percentage of heterocyst cells between 48 and 72 hours, complementation requires the differentiation of a normal pattern of heterocysts between 24 and 48 hours after nitrogen removal. Although not previously reported, it is common for the Δ*hetP* mutant strain to produce unusually short filaments. Such strains are said to have a fragmentation phenotype. This problematic phenotype was apparent when observing the Δ*hetP* mutants containing the plasmids carrying the 25, 50, 68, or 75 amino acid *hetP*-truncations. For these strains, the time of onset of heterocyst differentiation was recorded as well as the relative percentage of heterocyst cells observed. Due to the fragmentation phenotype it was not clear if a normal pattern of heterocyst cells was established. The results of the complementation study of the Δ*hetP* mutant are summarized in (Figure 4).

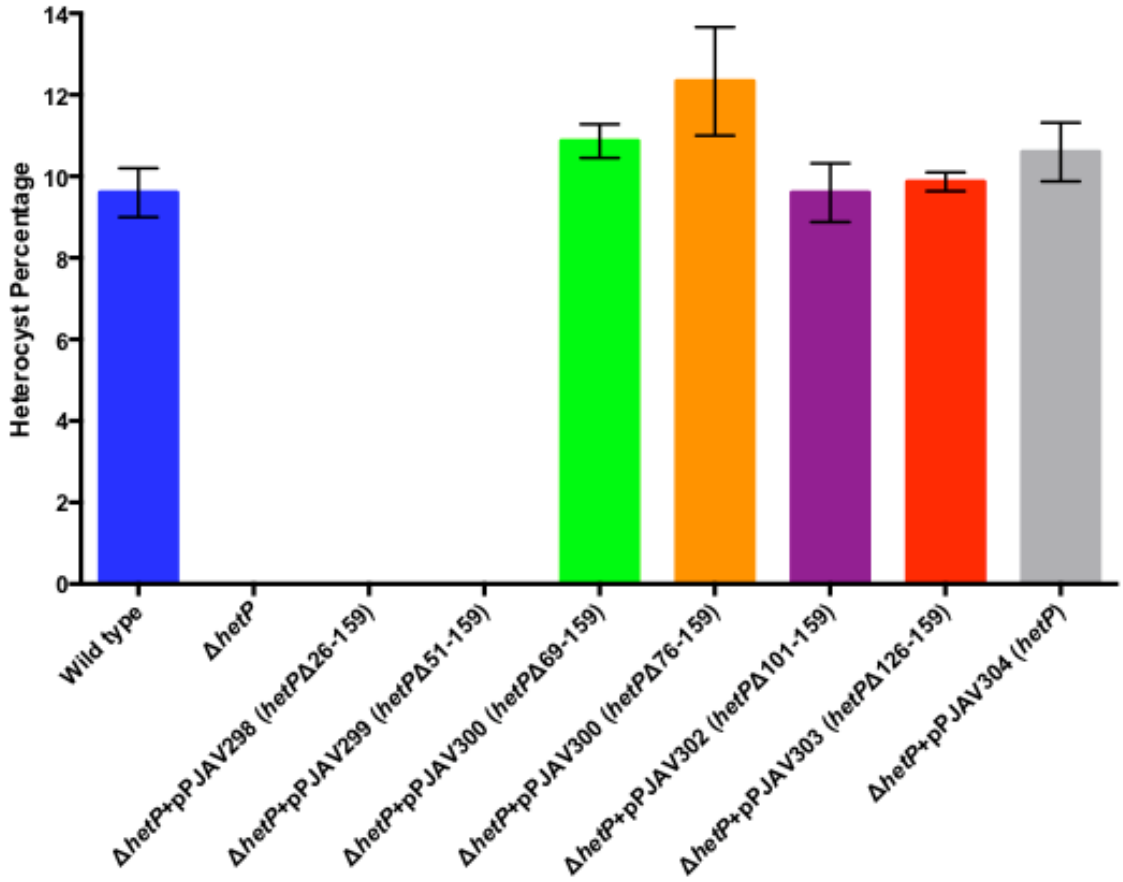

Figure 4: Heterocyst percentages of *hetP* truncation mutations present on a multicopy shuttle vector expressed in a Δ*hetP* strain, 24 hours after nitrogen removal.

The Δ*hetP* culture and those containing the 25 and 50 amino acid *hetP*-truncation plasmids did not form heterocyst cells in the absence of nitrate at 24 hours (Figures 4 and 5). Additionally, the strains containing these plasmids were highly fragmented and did not grow well in liquid medium. Conversely, the *hetP* mutant with plasmids encoding the 68 amino acid truncation or longer (75, 100, and 125) produced a number of heterocysts similar to that of the *hetP* mutant with a full-length version of *hetP*, by 24 hours after nitrogen starvation (Figure 5).

High fragmentation was observed in the strains carrying the 25, 50, 68 and 75 amino acid truncations. The high level of fragmentation seems to be, at least somewhat,

resolved in the strains carrying the *hetP*-100 and *hetP*-125 alleles. This result could indicate filament integrity as a second possible role of the HetP protein. Perhaps the N-terminal amino acids of the HetP protein play a role in heterocyst differentiation while the C-terminal end influences the filament integrity of *Anabaena*.

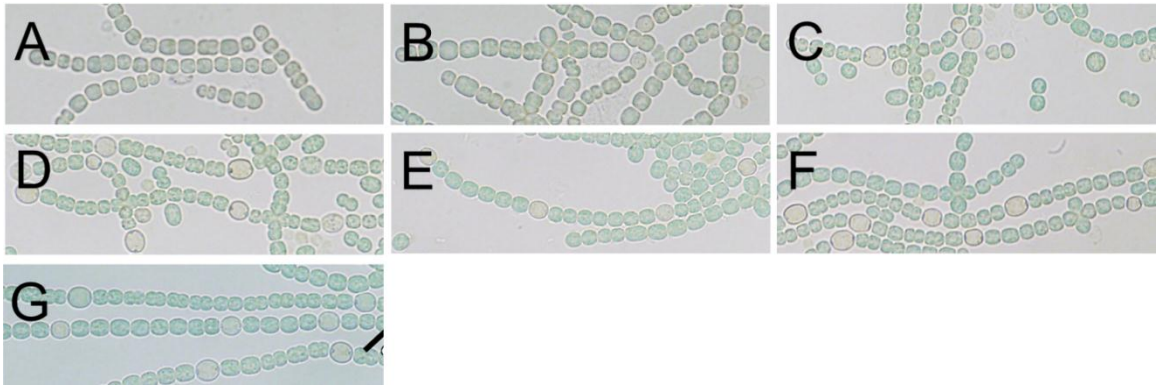

Figure 5: Δ*hetP* mutants containing vectors with the following *hetP* truncations: A) *hetP*-25 ; B) *hetP*-50; C) *hetP*-68 ; D) *hetP*-75 ; E) *hetP*-100 ; F) *hetP*-125 ; G) full-length *hetP*, 24 hrs after nitrogen removal.

The HetP truncation complementation experiments, described above, utilize multi-copy plasmids and therefore the resulting phenotypes may be attributed to the copy number of plasmids expressing the gene (truncation) of interest. To alleviate any role copy number may play in the complementation of the Δ*hetP* strain the same truncations were created in the chromosome. To accomplish this, suicide vectors (pPJAV232-237) carrying the *hetP* promoter and each of the six *hetP* truncations were introduced in a Δ*hetP* background. The resulting strains were observed for their ability to produce heterocysts 24 hours after nitrogen removal; micrographs of these strains are represented in (Figure 6).

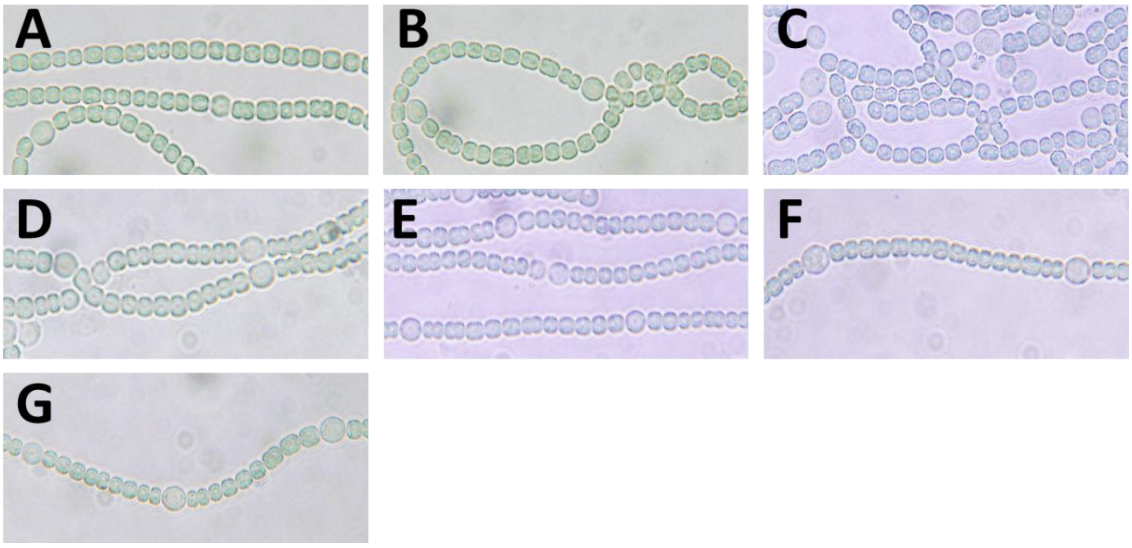

Figure 6: HetP chromosomal truncation mutants 24 hrs after nitrogen removal: A) *hetPΔ26-159*, B) *hetPΔ51-159*, C) *hetPΔ69-159*, D) *hetPΔ76-159*, E) *hetPΔ101-159*, F) *hetPΔ126-159*, G) $hetP_{full\text{-}length}$.

The observed phenotypes of the chromosomal insertions, of each of the HetP truncations, were very similar to those observed in the plasmid-based complementation study (Figure 6 and Figure 7). Namely, wild-type and near wild-type percentages of heterocysts were observed at 24 hours in strains *hetPΔ69-159*, *hetPΔ76-159*, *hetPΔ101-159*, and *hetPΔ126-159* representing the 68, 75, 100, and 125 amino acid truncations, respectively (Figure 6). Fragmentation was again observed in the strain coding for the first 68 amino acids of HetP (*hetPΔ69-159*); no fragmentation was observed in any of the other HetP-truncation mutants, including the 25, 50, and 75 amino acid truncations that displayed the fragmentation phenotype when expressed on a plasmid (Figure 5). The smallest HetP that was able to restore a wild-type percentage of heterocyst, at 24 hours after nitrogen removal, and maintain filament integrity was the *hetPΔ76-159* mutant (figures 6 and figure 7).

The strains encoding the 25 and 50 amino acid truncations, *hetPΔ26-159* and *hetPΔ51-159*, respectively, did not differentiate mature heterocysts, at 24 hours, although

what appear to be “pro-heterocyst” cells were observed. These cells have not lost the ability to auto-fluoresce. However, they do appear to be somewhat larger and rounder (characteristics of heterocyst cells) when compared to the neighboring vegetative cells. These strains do produce what appear to be mature heterocyst cells that lose auto-fluorescence and produce a polysaccharide envelope that stains with Alcian blue, by 96 hours after nitrogen removal. This finding is not significant in the analysis of the functional complementation of a Δ*hetP* mutant as it too produces a similar phenotype by this late time-point.

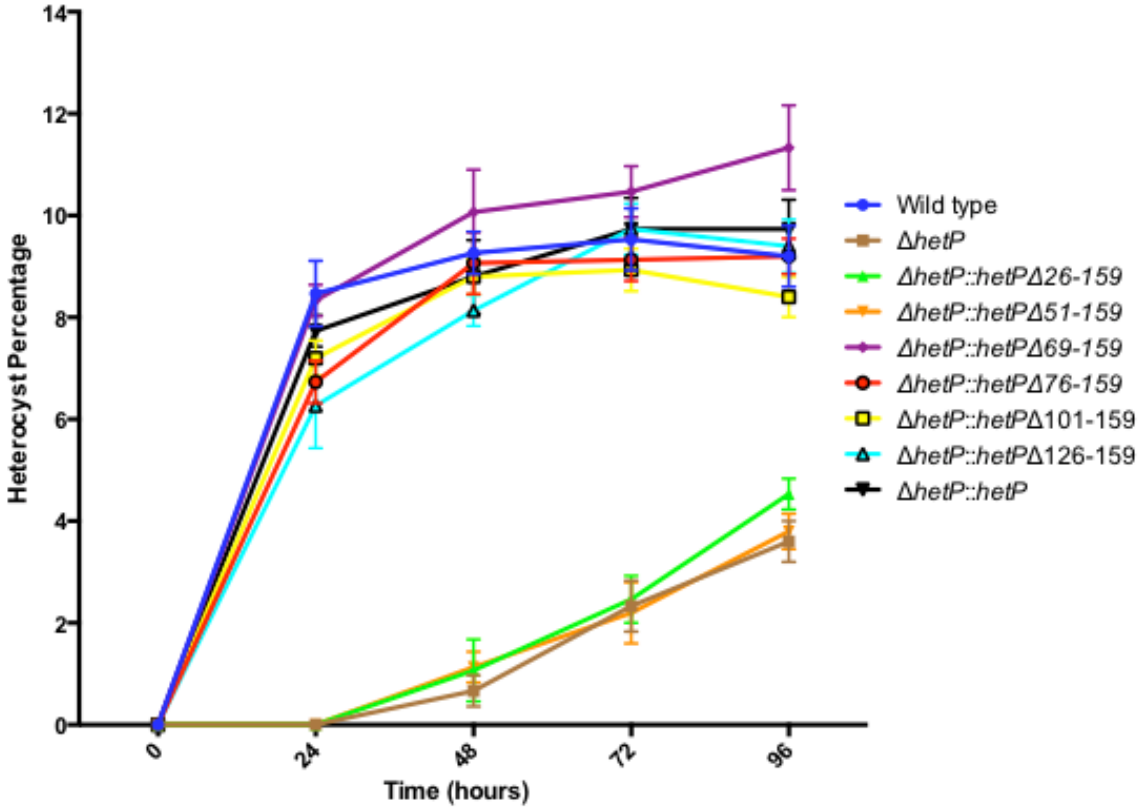

Figure 7: Heterocyst percentages, over time, of *hetP* truncation mutants

The Two Cysteine Residues of HetP

Two cysteine amino acids are present in the 159 amino acid HetP protein at positions 36 and 95. Cysteine residues are capable of creating disulfide bonds, which can be important in the tertiary and quaternary structures of proteins. To determine if the cysteine residues found in the HetP protein contribute to its function, mobilizable shuttle vectors (pPJAV305-307) carrying the *hetP* gene with cysteine-to-alanine mutations singly or at both of the 36 and 95 cysteine residues, driven by the *hetP* promoter, were introduced into wild-type and Δ*hetP* strains. The Δ*hetP* strain containing the plasmid with the $hetP_{C36A}$ mutation and the $hetP_{C36A/C95A}$ mutations produced no heterocyst cells in the absence of nitrogen (Figure 8). In contrast, the Δ*hetP* strain carrying the plasmid with the cysteine-to-alanine mutation at position 95 did form heterocysts in the absence of nitrogen (Figure 8). The result for the individual cysteine-to-alanine mutations at the 36 and 95 amino acid residues did not support the theory that the cysteine residues are involved in forming a disulfide bond within HetP. However, the results do indicate that the cysteine residue at position 36 is important for the function of HetP. It is possible that the cysteine residue is important in formation of inter-protein disulfide bonds, possibly involved in stabilization of a dimeric protein.

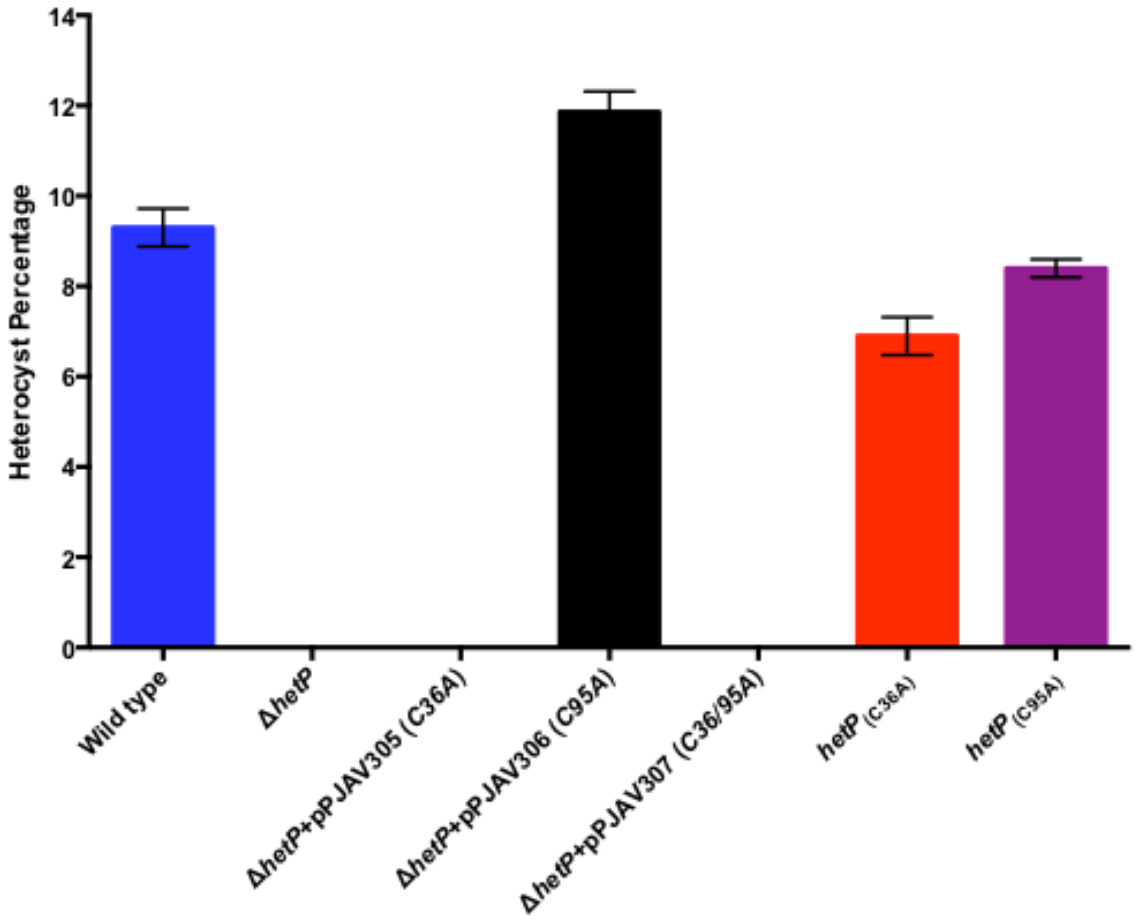

Figure 8: Heterocyst percentages, 48 hours after nitrogen removal, of wild-type, Δ*hetP*, Δ*hetP* carrying multicopy plasmids containing C-A mutations, and $hetP_{C36A}$ and $hetP_{C95A}$ mutants.

To determine if the observed phenotypes were a result of the HetP-cysteine mutations being expressed on a multi-copy vector, the mutations were introduced into the chromosome of a Δ*hetP* strain. Chromosomal mutants containing the C36A and C95A HetP substitutions yielded unexpected results. Both of the C36A and C95A HetP mutants produced near-wild-type percentages of heterocysts at 24 hours after nitrogen removal, reaching wild-type percentages by 48 hours (Figure 8 and Figure 9 (C&D)). Additionally, the heterocyst cells in both strains were efficiently stained with Alcian blue at 96 hours after nitrogen removal, suggesting that the exopolysaccharide layer of their heterocyst cells is present and intact (Figure 10 (B&C)). Interestingly, only the $hetP_{C95A}$

chromosomal mutant was capable of persisting on BG-11_0 media. Despite the discrepancy in heterocyst percentages of the HetP-C36A substitution expressed on a plasmid versus in the chromosome, the results indicate that this cysteine residue may play an important role in the function of HetP.

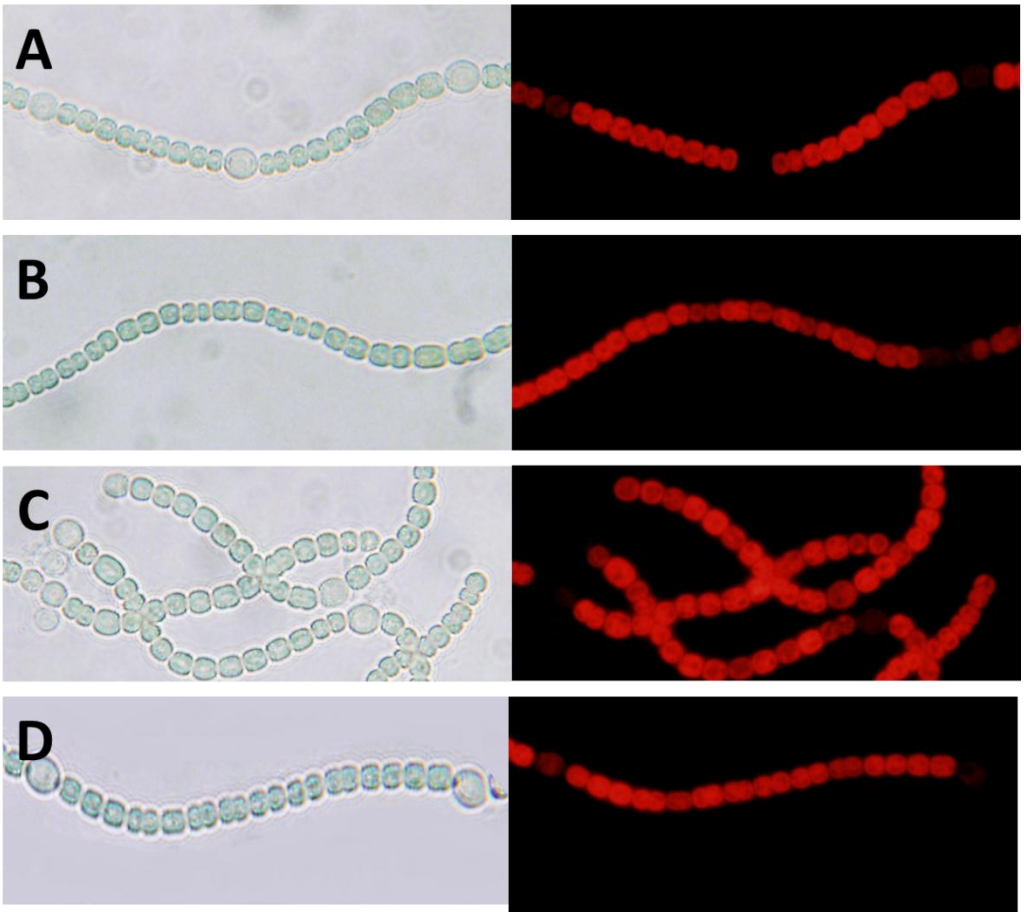

Figure 9: Light micrographs of bright field (left) and auto-fluorescence (right) of A) wild-type, B) Δ*hetP*, C) $hetP_{C36A}$, and D) $hetP_{C95A}$, 24 hours after nitrogen removal.

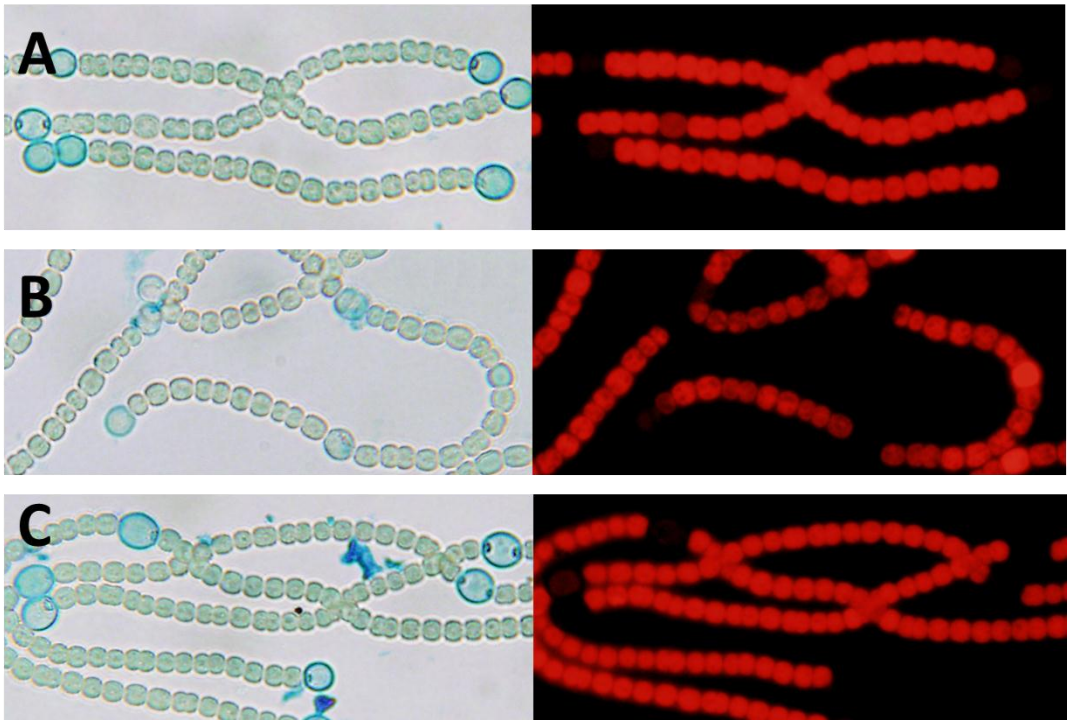

Figure 10: Light micrographs of bright field (left) and auto-fluorescents (right) of cells stained with Alcian blue, after 96 hours after nitrogen removal, in A) wild-type, B) *hetP*$_{C36A}$, and C) *hetP*$_{C95A}$ background strains.

CHAPTER 4. HOMOLOGUES OF HETP

hetP and *hetP*-homologue Mutant Strains

Due to the high level of similarity of the *hetP* homologues to the *hetP* gene, further characterization of each homologue was required for the investigation of their possible role in heterocyst differentiation and function. Overexpression vectors of each of the homologues suggested that at least two of the homologues, *hetP2* (alr2902) and *hetP3* (*alr3234*), may display some functional redundancy with the *hetP* gene (Higa, 2010). To investigate the role of the homologues in heterocyst formation, deletion strains were constructed and observed to determine relative contributions to heterocyst formation.

Clean mutations were made to create the following "single," "double," "triple," and "quadruple" deletion strains in *Anabaena*: Δ*hetP2*, Δ*hetP1,* Δ*hetP1*Δ*hetP2,* Δ*hetP*Δ*hetP1*, Δ*hetP*Δ*hetP2*, Δ*hetP*Δ*hetP3,* Δ*hetP*Δ*hetP1*Δ*hetP2*, Δ*hetP*Δ*hetP1*Δ*hetP3,* Δ*hetP*Δ*hetP2*Δ*hetP3* and Δ*hetP*Δ*hetP1*Δ*hetP2*Δ*hetP3*$_{sp/sm}$. All of the genes were cleanly deleted from the chromosome with the exception of the *hetP3* gene in the quadruple mutant. The *hetP3* gene in the quadruple *het*P mutant was interrupted with the insertion of a Sp^r/Sm^r cassette.

Single *hetP*-homologue Mutant Phenotypes

In the preliminary characterizations, the single mutant strains, Δ*hetP1* and Δ*hetP2,* generated a wild-type pattern of heterocyst cells upon nitrogen starvation (Figure 12). The Δ*hetP1* mutant was capable of supporting growth on solid BG-11_0 (media lacking a source of fixed nitrogen) and the heterocyst cells produced by this strain displayed a loss in autofluorescence and were stained with Alcian blue (results not shown). Interestingly, when plated on solid BG-11_0, Δ*hetP2* failed to grow. The

heterocysts of this strain appear to be mature when viewed under the light microscope and display the characteristic loss of auto-fluorescence (Figure 11A).

To further investigate the functionality of the heterocysts produced by Δ*hetP2*, a number of experiments were executed. First, the heterocysts stained with Alcian blue 96 hours after nitrogen removal (Figure 11B), suggesting that their exopolysaccharide layer is present and intact. Next, a promoter fusion to the nitrogen-fixing gene, *nifB*, was introduced on plasmid pPJAV295. Expression form the *nifB* promoter in the Δ*hetP2* strain appeared similar to that in wild type (Figure 11C). This suggests that the expression of at least one of the nitrogen-fixing genes is normal. Finally, to determine if Δ*hetP2* is capable of fixing atmospheric nitrogen, an acetylene reduction assay was performed. In this experiment, the culture is exposed to acetylene gas to determine if the bacterium is capable of reducing it to ethylene. This reduction is carried-out by the same enzymes that reduce di-nitrogen to ammonia. No acetylene reduction could be detected from with this strain (Figure 11D), suggesting that Δ*hetP2* is not capable of reducing nitrogen under atmospheric conditions.

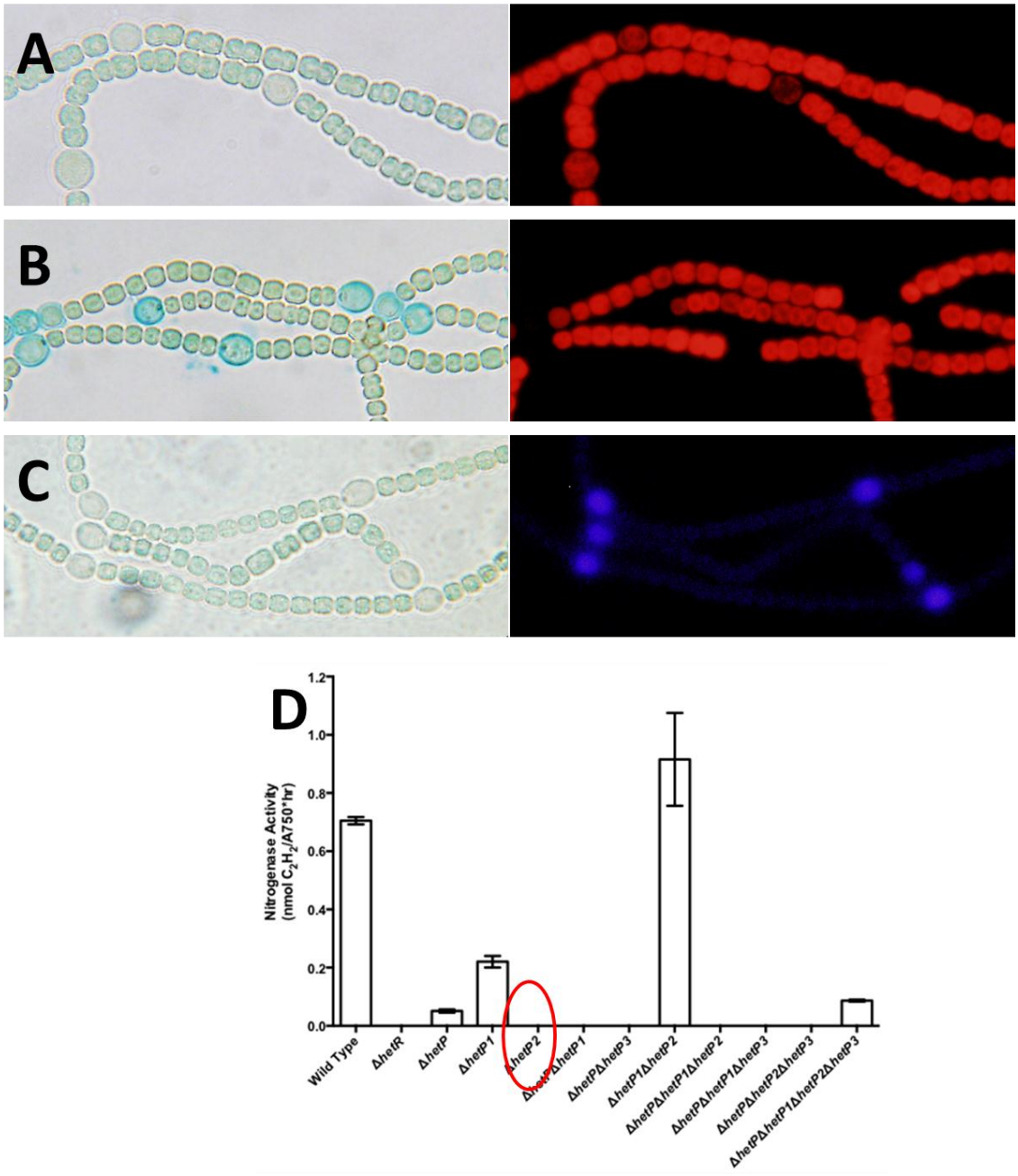

Figure 11: Δ*hetP2* (Δ*alr2902*) A) bright field (left) and autoflourescence (right) 24 hrs after nitrogen removal; B) Alcian blue stained (left) and autoflourescence (right) 96 hours after nitrogen removal; C) expressing pPJAV295 (PnifB-FbFP) bright field (left) and FbFP-flourescence (right); D) acetylene reduction assay.

Double *hetP*-homologue Mutant Phenotypes

The double mutant strains differentiate a similar percentage of heterocysts cells as the Δ*hetP* mutant, although their onset appears to be slightly enhanced, appearing by 48 hours after nitrogen removal (Figure 12).

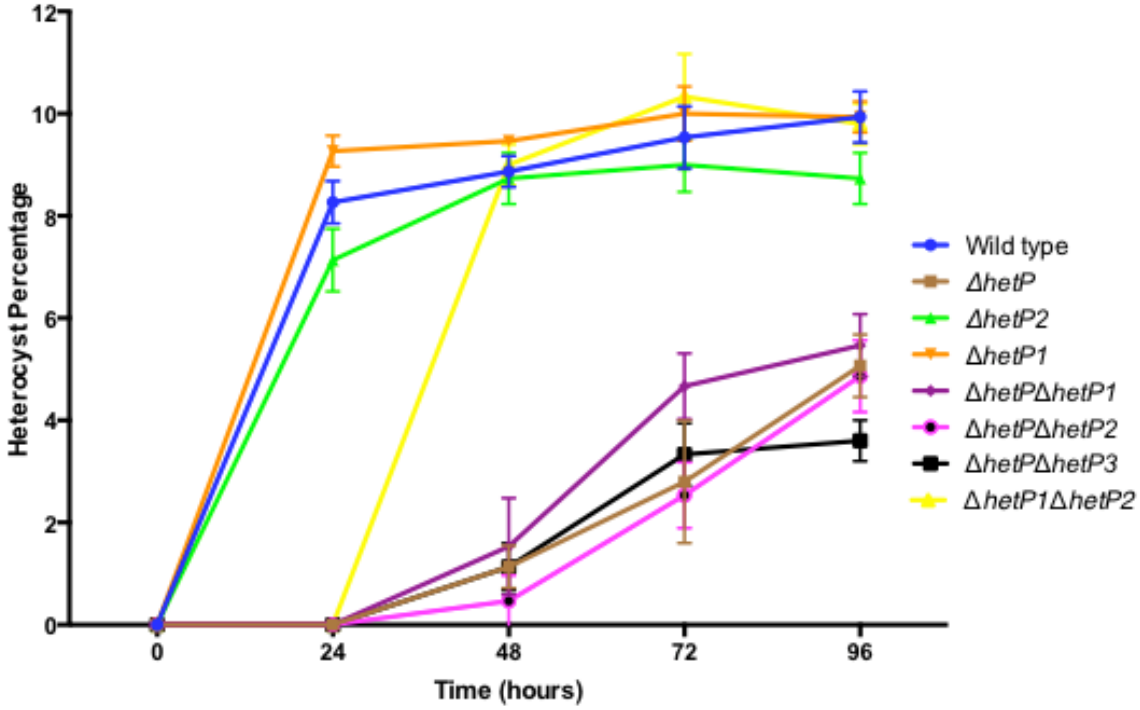

Figure 12: Heterocyst percentages, over time, of wild-type, Δ*hetP*, *hetP*2 homologue mutant, and *hetP*-*hetP*-homologue double mutants.

A double mutant, Δ*hetP1*Δ*hetP2*, was constructed and analyzed. This strain, with two of the three *hetP*-homologues cleanly deleted from the chromosome, displayed a wild-type pattern and percentage of heterocyst cells but not until 48 hours after nitrogen removal (Figure 12). Additionally, this strain was capable of growth on BG-11_0 media and was shown to fix nitrogen via an acetylene reduction assay (Figure 11D).

Triple *hetP*-homologue Mutant Phenotypes

The triple mutant strains appear to differentiate heterocysts at a percentage intermediate to that of the wild type and Δ*hetP* strains. Heterocysts in these strains appear by 48 hours after nitrogen removal, and peak to an average of 5% of heterocyst cells (Figure 13). The Δ*hetP* mutant was previously reported to differentiate 1-2% heterocyst cells; however, results of this study indicate that the Δ*hetP* strain is capable of differentiation 4-5% of heterocyst cells by 96 hours after nitrogen removal. The phenotypes of the triple mutants Δ*hetP*Δ*hetP1*Δ*hetP2* and Δ*hetP*Δ*hetP1*Δ*hetP3* appear to most closely resemble a Δ*hetP* phenotype at 96 hours. The triple mutant *hetP*Δ*hetP2*Δ*hetP3* appears to differentiate the highest percentage of heterocyst cells when compared to all three triple mutants constructed (Figure 13).

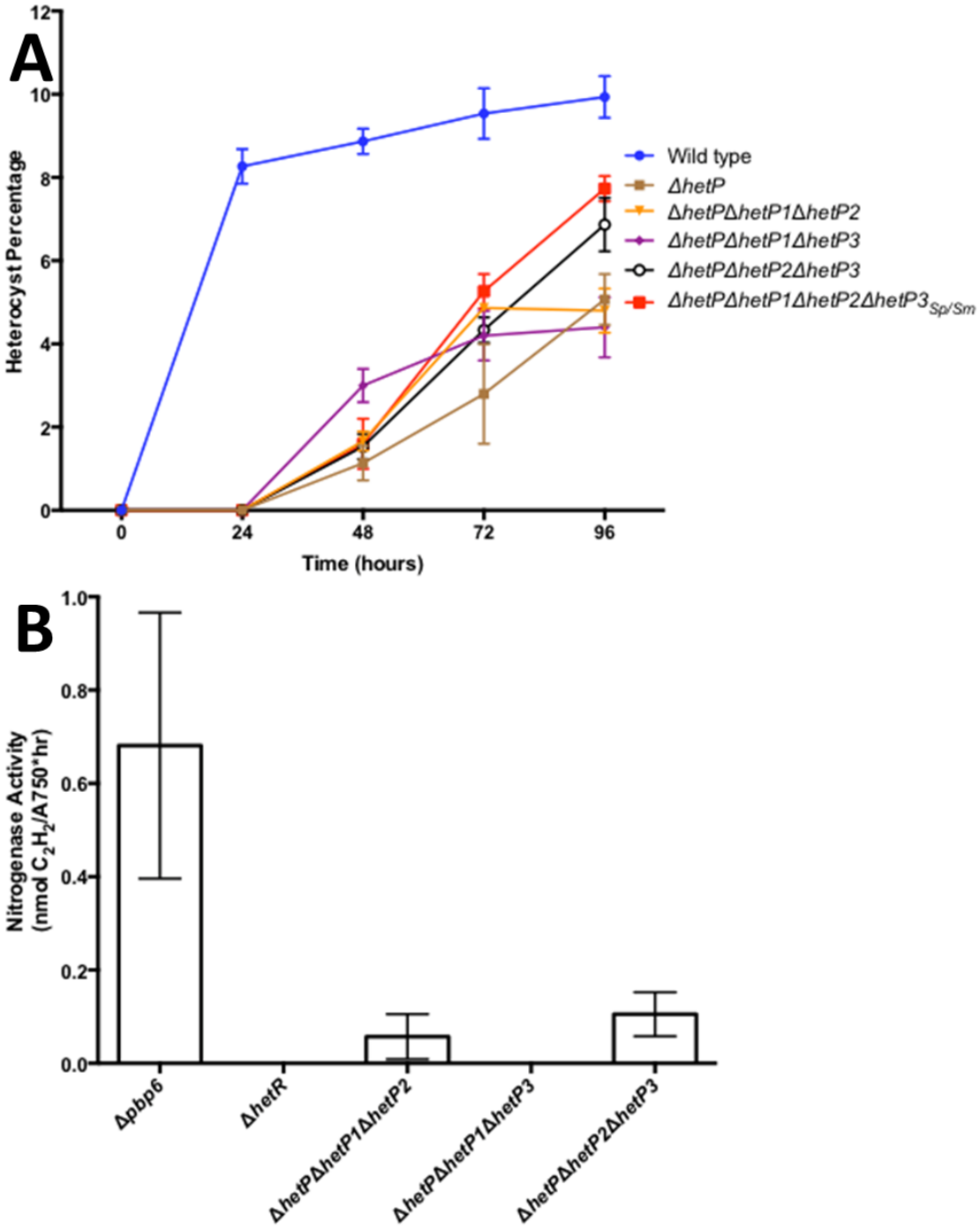

Figure 13: **A.** Heterocyst percentages, over time, of wild-type, Δ*hetP*, *hetP*-*hetP* homologue triple and quadruple mutants. **B.** Acetylene reduction assay performed under anoxic conditions.

In contrast to Δ*hetP* and the *hetP*-double mutant strains, the *hetP*-triple mutants frequently have a Mch phenotype. The heterocyst cells produced by the triple mutants

rarely resemble the large, round, heterocyst cells typical of the wild-type strains and, instead, appear much smaller in size, sometimes smaller than the neighboring vegetative cells. This phenotype is most extreme in the Δ*hetP*Δ*hetP1*Δ*hetP3* strain. However, these heterocyst-like cells display the classic loss of auto-fluorescence displayed by mature heterocysts (Figure 15). Δ*hetP*Δ*hetP1*Δ*hetP2* and Δ*hetP*Δ*hetP1*Δ*hetP3* triple mutant strains most closely resemble a Δ*hetP* strain, in terms of heterocyst percentages, at 96 hours after nitrogen removal. However, these strains produce percentages of heterocysts greater than the *het*P mutant between 48 and 72 hours. The triple mutant strain Δ*hetP*Δ*hetP2*Δ*hetP3* more closely resembles the quadruple mutant strain, having an intermediate percentage of heterocyst cells between that of the *hetP* strain and wild-type (Figure 16).

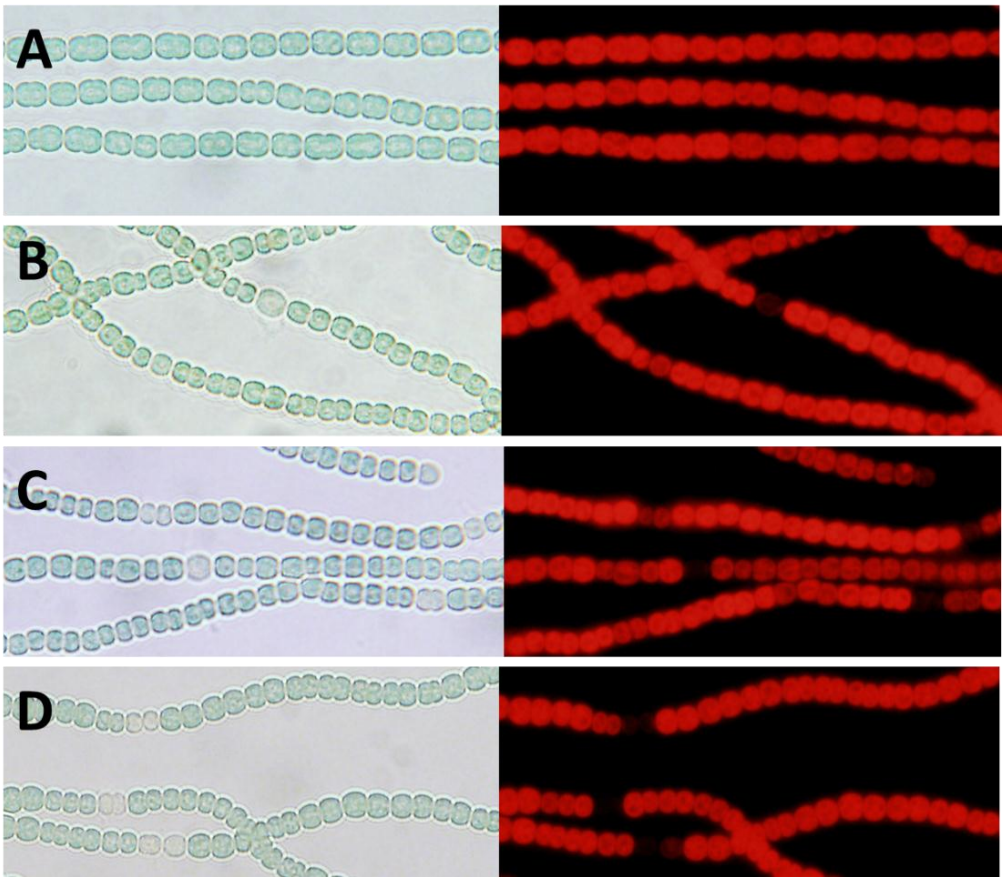

Figure 14: Bright field (left) and auto-fluorescent (right) micrographs of mutant strain *hetP*Δ*hetP1*Δ*hetP2* A) 0 hrs, B) 48 hrs, C) 72 hrs, and D) 96 hrs after nitrogen starvation.

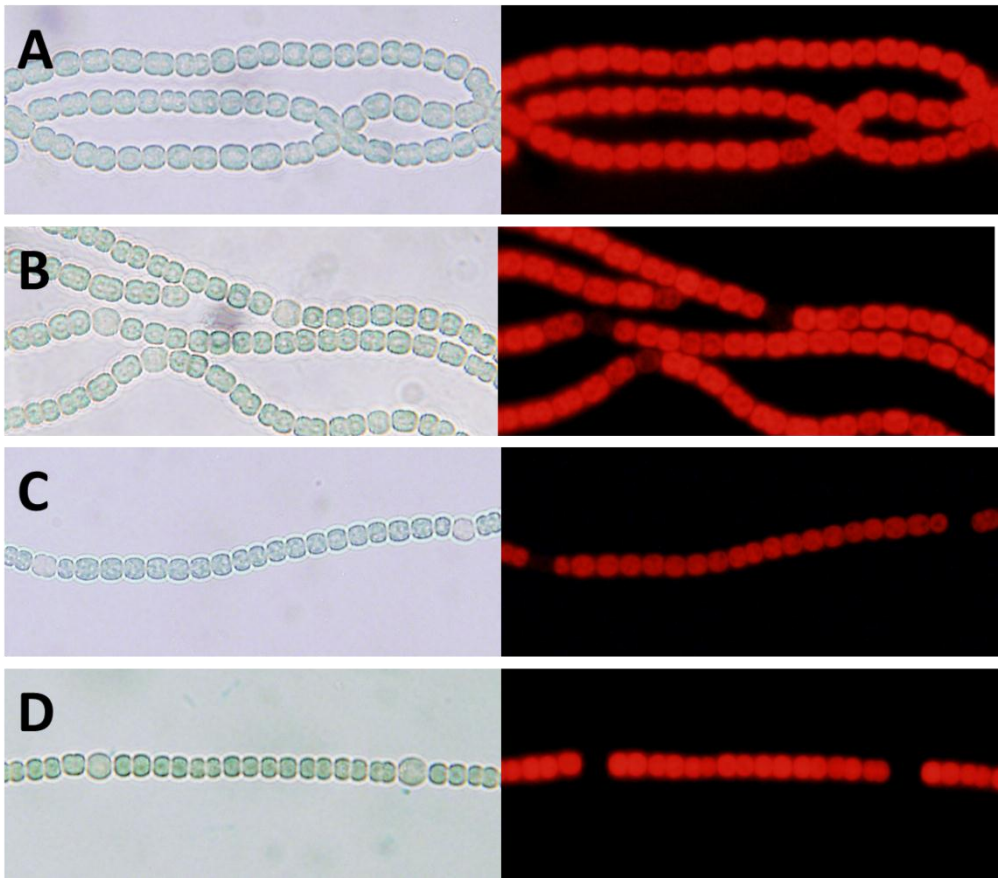

Figure 15: Bright field (left) and auto-fluorescent (right) micrographs of mutant strain *hetP*Δ*hetP1*Δ*hetP3* A) 0 hrs, B) 48 hrs, C) 72 hrs, and D) 96 hrs after nitrogen starvation.

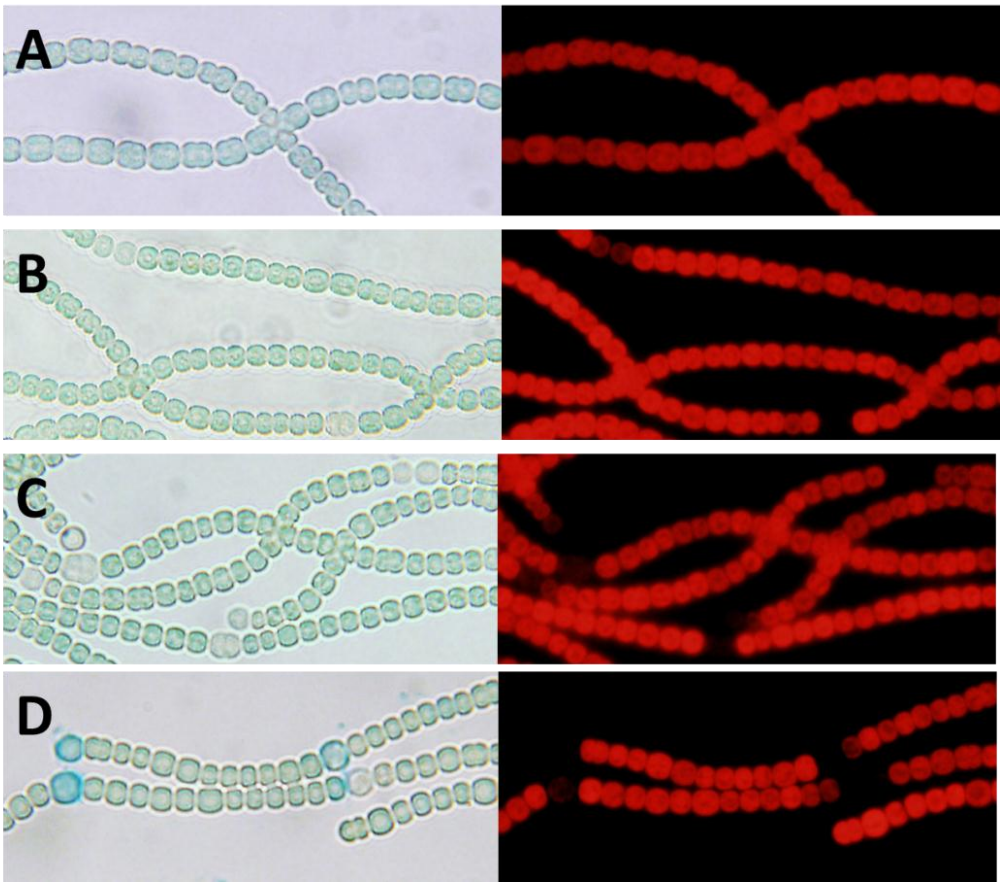

Figure 16: Bright field (left) and auto-fluorescent (right) micrographs of mutant strain *hetP*Δ*hetP2*Δ*hetP3* A) 0 hrs, B) 48 hrs, C) 72 hrs, and D) 96 hrs after nitrogen starvation (shown stained with Alcian blue).

The heterocyst cells of the triple mutants were stained with Alcian blue to determine if they contain the exopolysaccharide layer, important in creating a microoxic environment necessary for proper functioning of the nitrogenase enzyme. The heterocyst cells of the triple mutant Δ*hetP*Δ*hetP1*Δ*hetP3* failed to bind the Alcian blue stain 96 hours after nitrogen removal, further suggesting that these heterocyst cells may not be mature (Figure 17C). The exopolysaccharide layers of the remaining triple mutants appear to be intact as indicated by the retention of the Alcian blue stain (Figure 17).

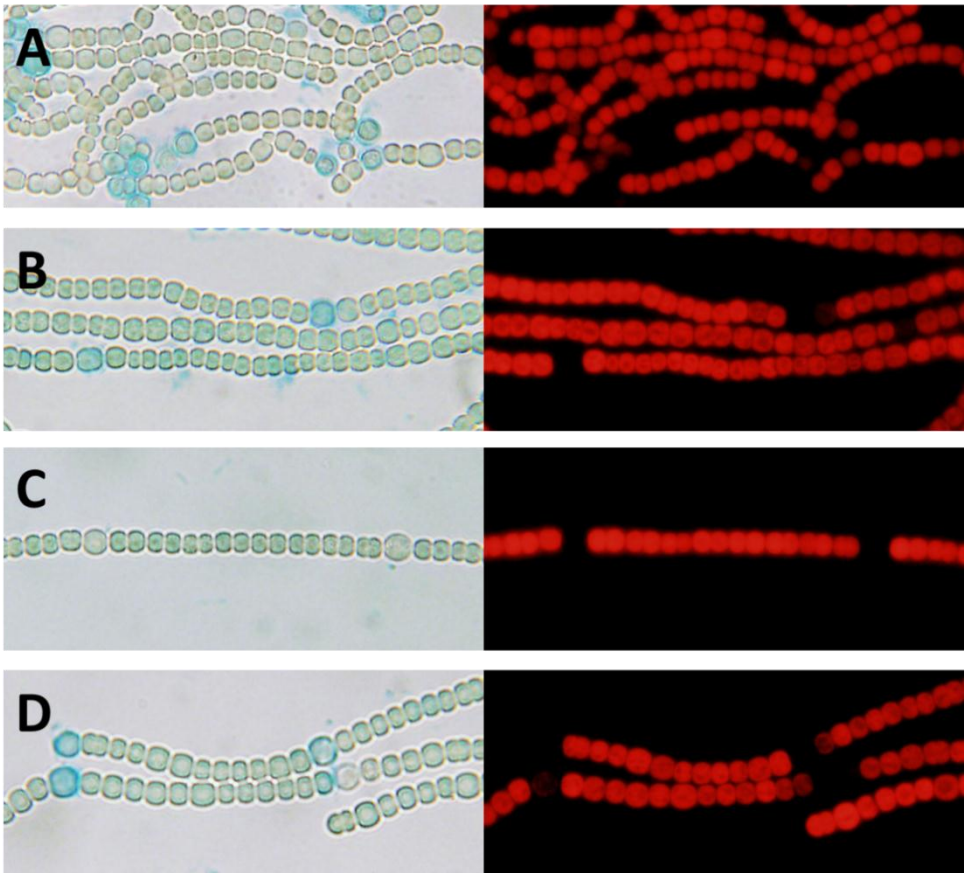

Figure 17: Light micrographs, bright field (left) and autofluorescence (right), of A) Δ*hetP*, B) Δ*hetP*Δ*hetP1*Δ*hetP2*, C) Δ*hetP*Δ*hetP1*Δ*hetP3*, and D) Δ*hetP*Δ*hetP2*Δ*hetP3* after staining with Alcian blue, 96 hours after nitrogen removal.

The triple mutants Δ*hetP*Δ*hetP1*Δ*hetP2* and Δ*hetP*Δ*hetP2*Δ*hetP3* are capable of limited growth on solid media lacking a source of fixed nitrogen. These strains support some growth on BG-11_0 media, however brown and die shortly thereafter; however, the triple mutant Δ*hetP*Δ*hetP1*Δ*hetP3* is not capable of growth on this type of media. No acetylene reduction was detected under oxic conditions for any of the *hetP*-triple mutants (Figure 11D), despite Δ*hetP*Δ*hetP1*Δ*hetP2* and Δ*hetP*Δ*hetP2*ΔhetP3 apparent slight growth on BG-11_0 media. Acetylene reduction was, however, detected in the triple mutant strains Δ*hetP*Δ*hetP1*Δ*hetP2* and Δ*hetP*Δ*hetP2*Δ*hetP3* under anoxic conditions

(Figure 13B). This suggests that there may be a defect in the membranes of the heterocyst cells and that the nitrogenase enzymes are present and functional.

Quadruple *hetP*-homologue Mutant Phenotype

The quadruple mutant was created to eliminate the functions of *hetP* and its three homologues, all together. The mutant was created by replacing most of the coding sequence of *hetP3* (*alr3234*) with a Sp/Sm resistance cassette in the previously constructed Δ*hetP*Δ*hetP1*Δ*hetP2* mutant strain. No heterocysts were observed in the strain 24 hours after nitrogen removal. However, the quadruple mutant produced a higher percentage of heterocyst cells when compared to the Δ*hetP* mutant by 48 hours of nitrogen starvation (Figure 13). The mutant strains, regardless of the combination of deleted genes, do not reach wild-type percentages of heterocysts after 96 hours of nitrogen starvation. However, there appears to be a correlation between increased heterocyst percentages and the combination of the *hetP* homologues that are deleted from the Δ*hetP* starting strain, with the quadruple mutant producing the highest percentage of heterocyst cells when compared to the other *hetP* homologue mutant strains.

The heterocyst cells formed in the quadruple mutant 96 hours after nitrogen starvation appear to take on a variety of sizes ranging from typical sized heterocysts to cells similar in size to vegetative cells (Figure 18). Due to this occurrence, it is possible that some heterocyst cells may be misrepresented as vegetative cells during cell counts, which are typically performed only under the bright field condition. Occasionally, a Mch phenotype is observed but more commonly doublets of heterocyst can be viewed along with singular heterocyst cells throughout a filament. Oddly, what appear to be septa are

sometimes observed within cells that appear to be heterocysts (Figure 18). Heterocyst cells, as mentioned previously, are terminally differentiated and are not known to divide.

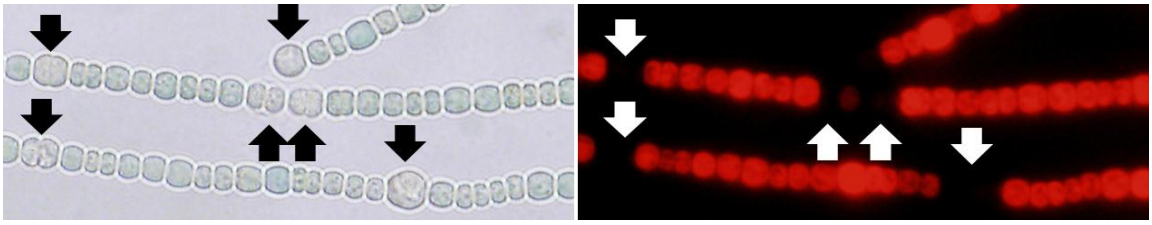

Figure 18: Light micrographs, bright field (left) and auto-fluorescent (right), of mutant strain Δ*hetP*Δ*hetP1*Δ*hetP2*ΔhetP3$_{Sp/Sm}$ 96 hours after nitrogen starvation. Arrows indicate heterocyst-like cells

Properties of the Quadruple *hetP* Mutant Strain

Due to the abnormal patterning of heterocyst cells observed in the quadruple mutant strain, a P$_{patS}$-GFP transcriptional reporter construct was introduced on plasmid pAM1951 to determine if a wild-type expression of the early patterning gene, *patS*, is observed. In the wild-type background, the GFP reporter construct produced fluorescence at approximately every tenth cell of the filament by six hours after nitrogen starvation. In the *hetP* mutant and in the quadruple mutant, overall patterning appears to be intact, but resolution of expression of *patS* to a single cell is not complete (Figure 19). The fluorescence was also observed in the mature heterocyst cells up to 96 hours after nitrogen removal (Data not shown).

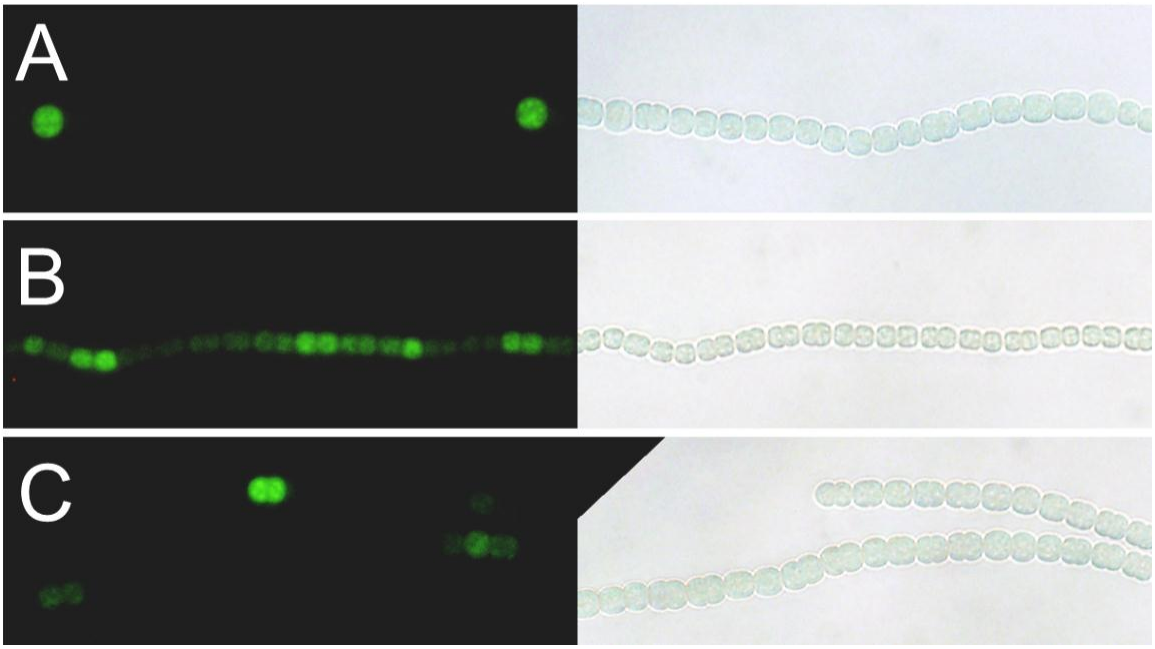

Figure 19: GFP (left) and bright field (right), $P_{patS\text{-}GFP}$ reporter fusion 18 hours post nitrogen removal in A) wild-type , B)Δ*hetP*, and C) Δ*hetP*Δ*hetP1*Δ*hetP2*Δ*hetP3*$_{Sp/Sm}$.

To investigate what appear to be possible division planes in the heterocyst cells of the quadruple mutant (Figure 18), a yellow fluorescent reporter protein was fused to a known division plane protein, FtsZ, and introduced on a plasmid. FtsZ is a protein known to play a key role in cell division, forming what is known as a "Z-ring" in the cell. It is thought to participate in cell division by a "draw-string" mechanism, cinching the midcell region until two daughter cells arise. In a wild-type strain, the FtsZ translational fusion is visualized as an accumulation of YFP at the division plane of the dividing cell (Figure 20A). When the plasmid pLMC115, which carries the FtsZ-YFP fusion, was introduced to the quadruple mutant strain, no clear Z-Rings were observed; instead, small yellow puncta were seen throughout both the vegetative and heterocyst cells, at 48 hours after nitrogen removal (Figure 20C). The cells appear to be dividing, as indicated by the growth of the filament, despite the lack of a visualized FtsZ-ring. A similar result was visualized in the Δ*hetP* strain, carrying the same plasmid (Figure 20B).

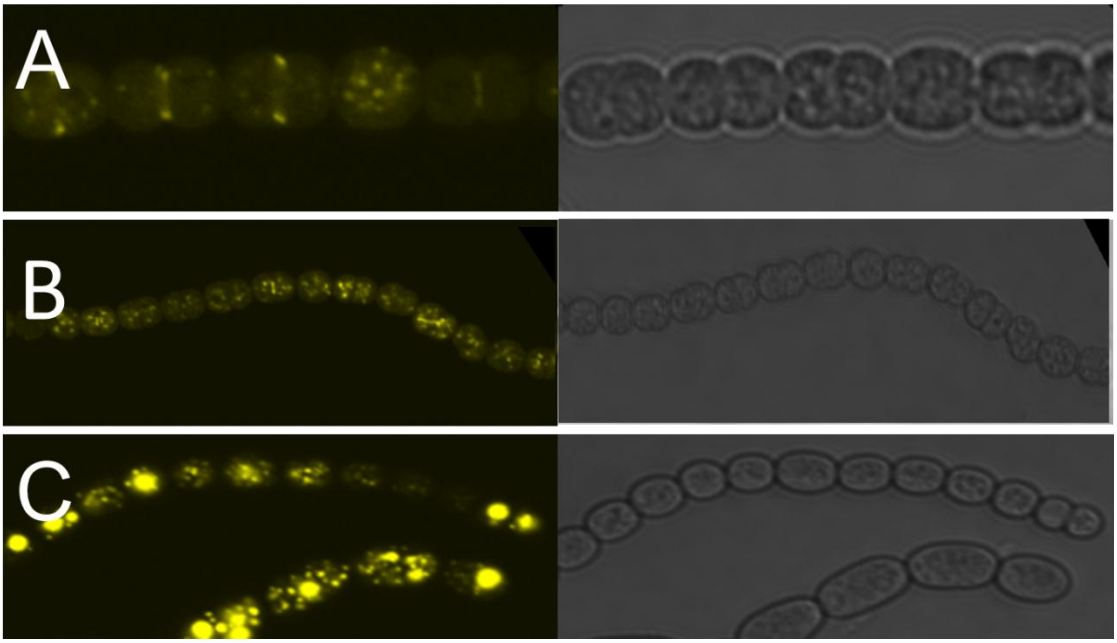

Figure 20: Yellow fluorescence (left) and bright field (right) of A) Wild-type, B) Δ*hetP* , and C) Δ*hetP*-quadruple mutant, carrying a YFP translational fusion to *ftsZ* on plasmid pLMC115 at 48 hours after nitrogen removal.

Heterocyst cells in the quadruple mutant were stained with Alcian blue, after 96 hours of growth in nitrogen deficient media, to determine if their exopolysaccharide layer is intact. The heterocysts in the quadruple *hetP* mutant take up the stain, suggesting that they produce the exopolysaccharide layer typical of wild-type heterocyst cells (Figure 21).

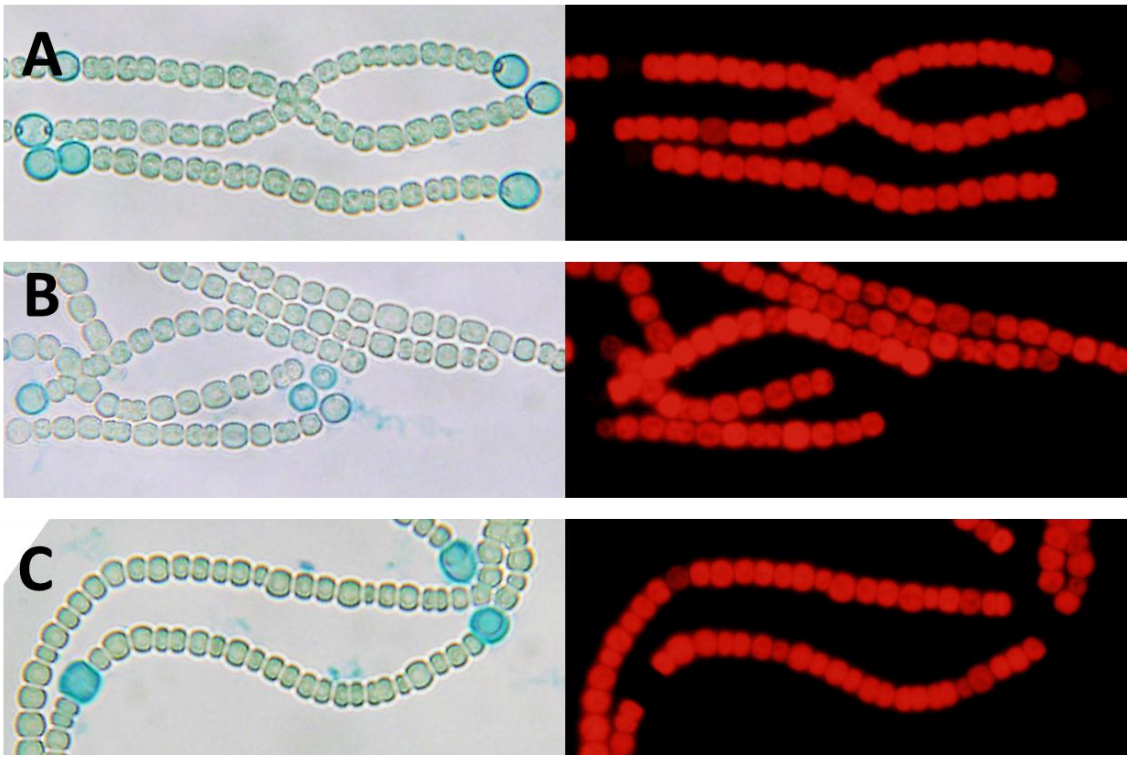

Figure 21: Micrograph showing heterocyst cells stained with Alcian blue (left) and loss of autofluorescence (right) of strains A) PCC 7120, B) Δ*hetP*, and C) Δ*hetP*Δ*hetP1*Δ*hetP2*Δ*hetP3*$_{Sp/Sm}$.

To investigate the expression of the heterocyst-specific nitrogenase gene, *nifB*, the promoter region of *nifB* was transcriptionally fused to FbFP (Flavin blue fluorescent protein) and introduced into the quadruple HetP mutant on plasmid pPJAV295. The *nifB* gene was expressed in the heterocysts of both the wild type and quadruple *hetP* mutant (Figure 22). Expression of *nif*B was also observed in the heterocysts of the *hetP* mutant (data not shown).

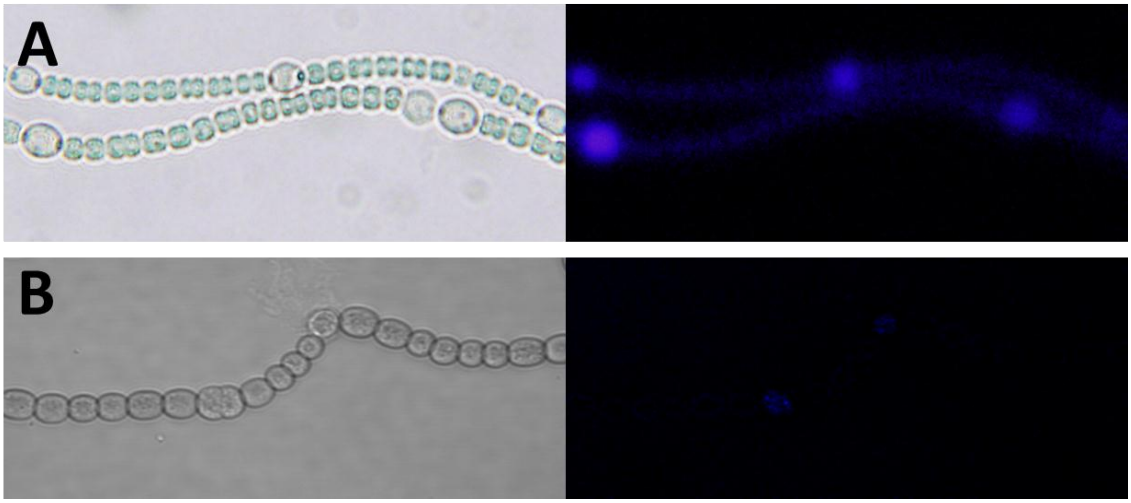

Figure 22: Bright field (left) and FbFP fluorescence (right) of A) wild type and B) Δ*hetP*Δ*hetP1*Δ*hetP2*Δ*hetP3*$_{Sp/Sm}$ carrying plasmid pPJAV295, 168 hrs after nitrogen removal.

Single, double, and triple mutants of *hetP* and the *hetP*-homologues were created to investigate their overall roll in heterocyst function and formation. No simple relationships between *hetP* and its homologues were revealed from the experiments conducted. An overall summary of the results of these experiments has been outlined in Table 5, below. Future experiments must be conducted to elucidate the intricate relationships *hetP* and its homologues hold in the roll of heterocysts function and formation.

Table 5: Summary of *hetP* and *hetP*-homologue mutant strain experiments. ND = not done

Mutant Strains	**Growth N- (0-5)**	**Acetylene Reduction (+/-)**	**Alcian Blue Stain**	**Expression of *nifB*-FbFP**	**Expression of P*patS*-GFP**
Δ*hetP*	3	+	+	+	+ (8hrs)
Δ*hetP1*	4	ND	+	ND	ND
Δ*hetP2*	0	-	+	+	ND
Δ*hetP1*Δ*hetP2*	5	+	+	ND	ND
Δ*hetP*Δ*hetP1*	3	-	+	ND	ND
Δ *hetP*Δ*hetP2*	3	ND	+	ND	ND
Δ*hetP*Δ*hetP3*	3	-	+	ND	ND
Δ*hetP*Δ*hetP1*Δ*hetP2*	2	-	+	ND	ND
Δ*hetP*Δ*hetP1*Δ*hetP3*	0	-	-	ND	ND
Δ*hetP*Δ*hetP2*Δ*hetP3*	2	-	+	ND	ND
Δ*hetP*Δ*hetP1*Δ*hetP2*Δ*hetP3*$_{sp/sm}$	4	+	+	+	+ (8hrs)

Expression of the *hetP*-homologues

To investigate the expression of each of the *hetP* homologues, transcriptional fusions to GFP were made to the promoter regions of *hetP*1, *hetP2*, and *hetP3* on plasmids pKLH103, pKLH104, and pKLH101, respectively. No known transcriptional start points (Tsps) of these genes have been identified (Muro Pasteor, 2011). Upstream DNA of each of the homologues was fused to GFP and observed in various background strains as outlined in Table 6.

Table 6: Expression of the *hetP* homologues in various background strains.

Background Strains	pKLH103 (P*hetP1*-GFP)	pKLH104 (P*hetP2*-GFP)	pKLH101 (P*hetP3*-GFP)
7120	Very low level of expression detected (slightly above background), 12 hrs N-. Expression was very low but appeared slightly stronger in heterocyst cells at 24 hrs N-	No expression detected	No expression detected
Δ*patA*	Very low level of expression detected (slightly above background), 12 hrs N-	No expression detected	No expression detected
Δ*hetR*	Very low level of expression detected (slightly above background), 12 hrs N-	No expression detected	No expression detected
Δ*hetF*	Very low level of expression detected (slightly above background), 12 hrs N-	No expression detected	No expression detected
Δ*hetP*	Expression was detected at 0hrs N- in most cells	No expression detected	Expression was detected at 8 hrs N- in all cell types. Expression peaked between 16 and 24 hrs N-
Δ*hetP*Δ*hetP1*	Expression was detected at 0hrs N- in all cell types. By 48 hrs N- expression appeared brighter approximately every 10-15 cells. At 72 hrs N- expression was prominent in heterocyst cells.	No expression detected	Expression was detected at 0hrs N- in all cells and in all cell types by 24 hrs N-
Δ*hetP*Δ*hetP2*	Expression was detected at 0hrs N- in all cell types. By 48 hrs N- expression appeared brighter approximately every 10th-15th cell. At 72 hrs N- expression was prominent in heterocyst cells with lowered expression in vegetative cells.	No expression detected	Expression was detected at 0hrs N- in all cells and in all cell types by 24 hrs N-

Δ***hetP*Δ*hetP3***	Expression was detected at 0hrs N- in all cell types. By 48 hrs N- expression appeared brighter approximately every 10-15 cells. At 72 hrs N- expression was prominent in heterocyst cells.	No expression detected	Expression was detected at 0hrs N- in all cells and in all cell types by 24 hrs N-

Expression of *hetP1*, from plasmid pKLH103, was detected at very low levels (slightly above background levels of GFP) in wild-type, Δ*patA*, Δ*hetF*, and Δ*hetR* at 12 hours after nitrogen removal (Table 6). In contrast, expression of *hetP1* in the Δ*hetP* mutant was strong at 0hrs after nitrogen removal, suggesting that *hetP* may be a repressor of *hetP1* expression (Figure 23). Expression of *hetP1* was also strong in the double *hetP*-homologue strains. Expression from these strains appeared fairly uniform in vegetative and heterocyst cells at 24 hours after nitrogen removal. However, at later time points expression seemed to increase in and then partially localize to heterocyst cells at 48 and 72 hours, respectively (Figures 24, 25, and 26). Evidence suggests that *hetP1* is not positively auto-regulated; however, there appears to be some correlation between increased expression in heterocyst cells and the lack of *hetP* in combination with each of its homologues.

No expression from plasmid pKLH104, carrying the upstream DNA of *hetP2* fused to GFP was detected in any background. This gene does not appear to be in an operon, and it is possible that there is a Tsp in this upstream region; however, expression is too low to detect from this construct.

Expression of *hetP3* was detected in strains lacking *hetP*, by 8 hours after nitrogen removal and appeared to peak at 24 hours (Table 6). No expression was detected in the wild-type strain (or other background strains containing *hetP*), suggesting that *hetP*

may be acting as a transcriptional repressor of *hetP3*. The data also suggests that *hetP3* is not positively auto-regulated, as expression in a strain lacking *hetP3* is similar to the other double-*hetP* homolog mutant strains (Δ*hetP*Δ*hetP1* and Δ*hetP*Δ*hetP3*). Expression detected in these strains appeared fairly uniform in all cells and in all cell types, at each of the time points (Figures 27, 28, and 29).

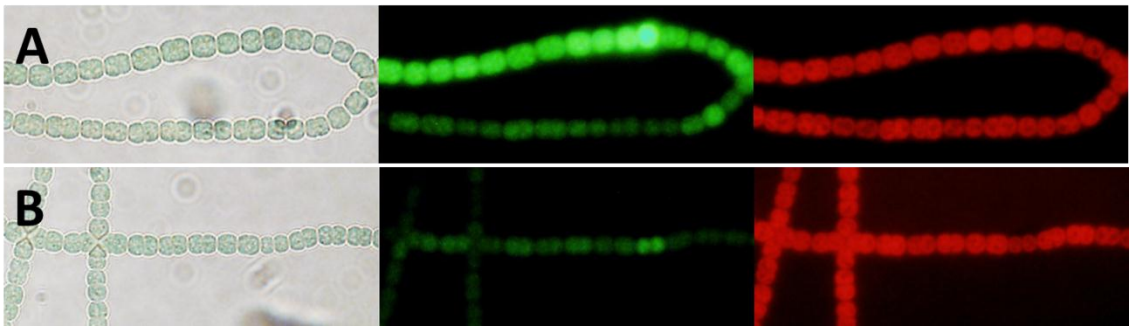

Figure 23: Micrographs (bright field, green fluorescence, autofluorescence) of Δ*hetP* carrying plasmids A) pKLH101 (P_{hetP3}-GFP) and B) pKLH103 (P*hetP1*-GFP), 24 hrs after nitrogen removal.

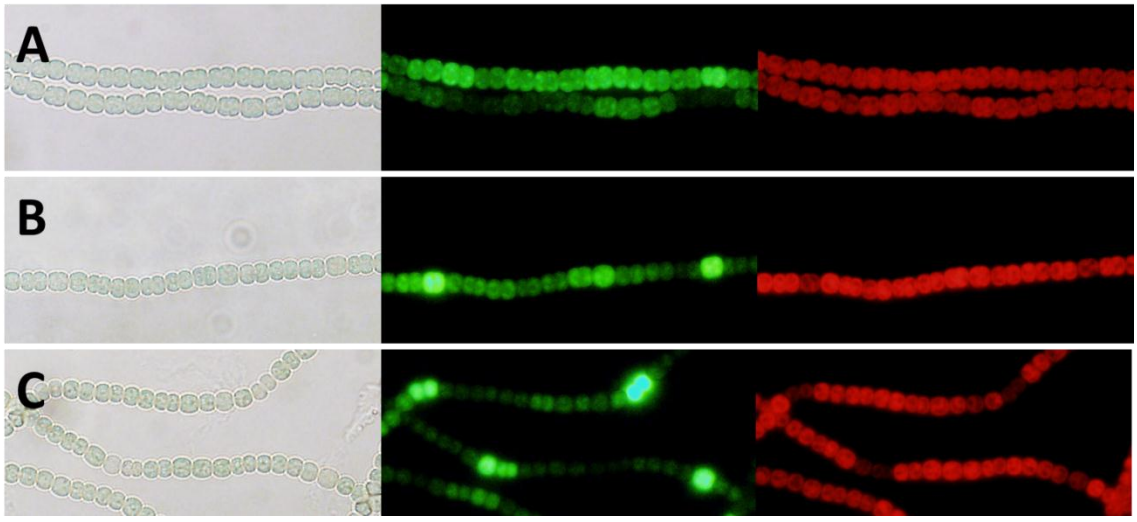

Figure 24: Micrographs (bright field, green fluorescence, autofluorescence) of Δ*hetP*Δ*hetP1* carrying plasmid pKLH103 (P_{hetP1}-GFP) A) 24 hrs, B) 48 hrs, and C) 72 hrs after nitrogen removal.

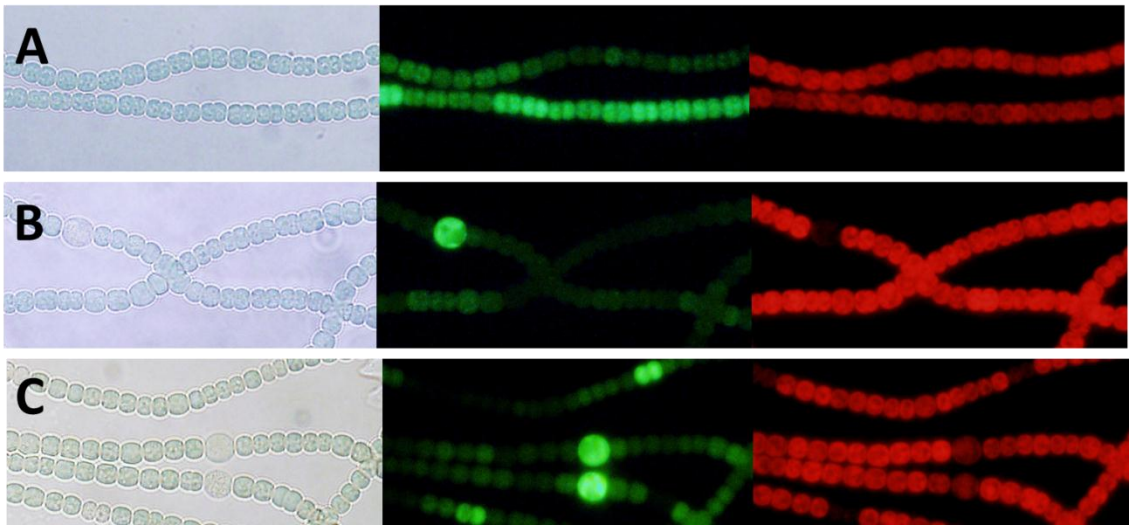

Figure 25: Micrographs (bright field, green fluorescence, autofluorescence) of Δ*hetP*Δ*hetP2* carrying plasmid pKLH103 (P_{hetP1}-GFP) A) 24 hrs, B) 48 hrs, and C) 72 hrs after nitrogen removal.

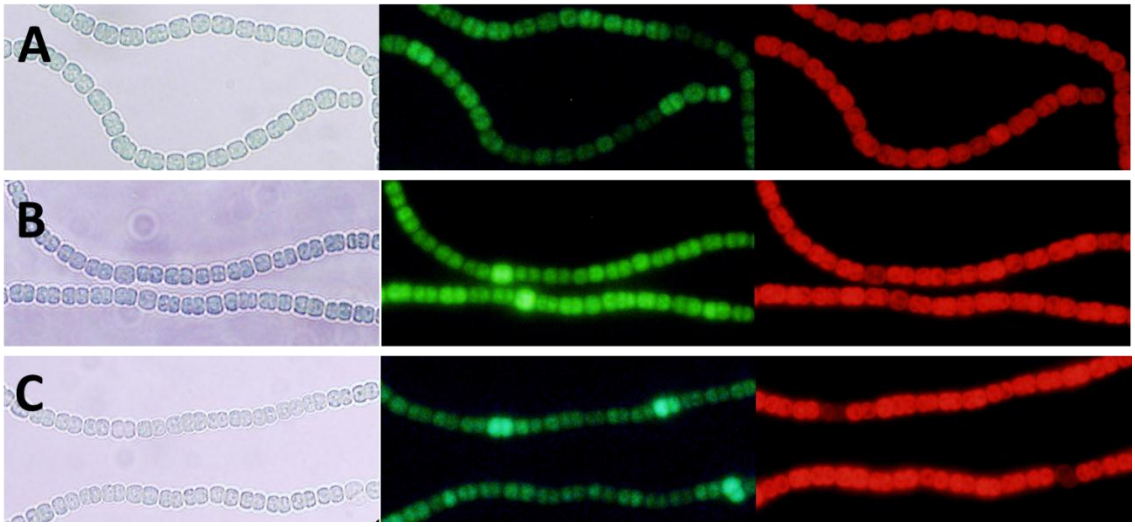

Figure 26: Micrographs (bright field, green fluorescence, autofluorescence) of Δ*hetP*Δ*hetP3* carrying plasmid pKLH103 (P_{hetP1}-GFP) A) 24 hrs, B) 48 hrs, and C) 72 hrs after nitrogen removal.

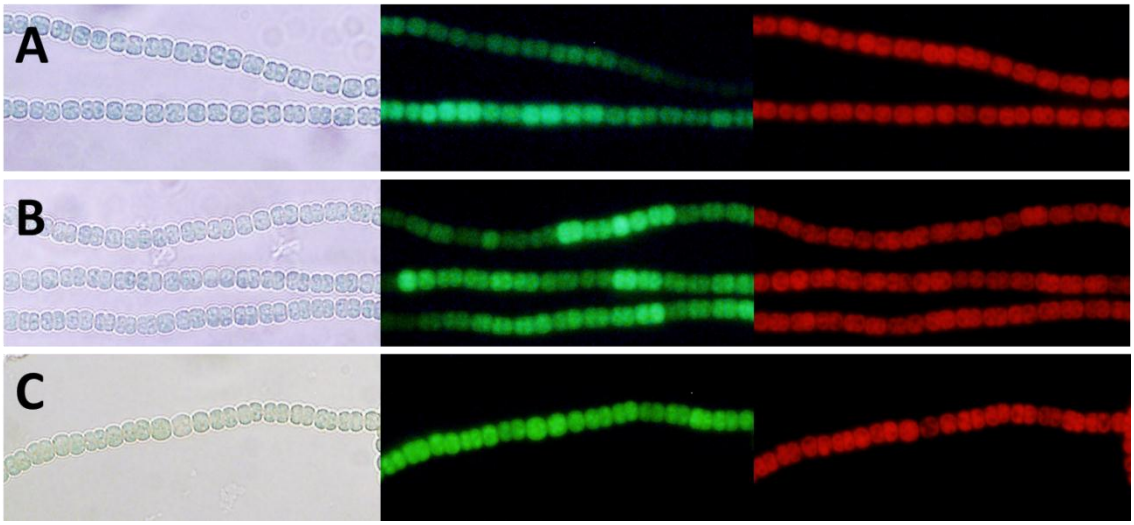

Figure 27: Micrographs (bright field, green fluorescence, autofluorescence) of Δ*hetP*Δ*hetP1* carrying plasmid pKLH101 (P_{hetP3}-GFP) A) 24 hrs, B) 48 hrs, and C) 72 hrs after nitrogen removal.

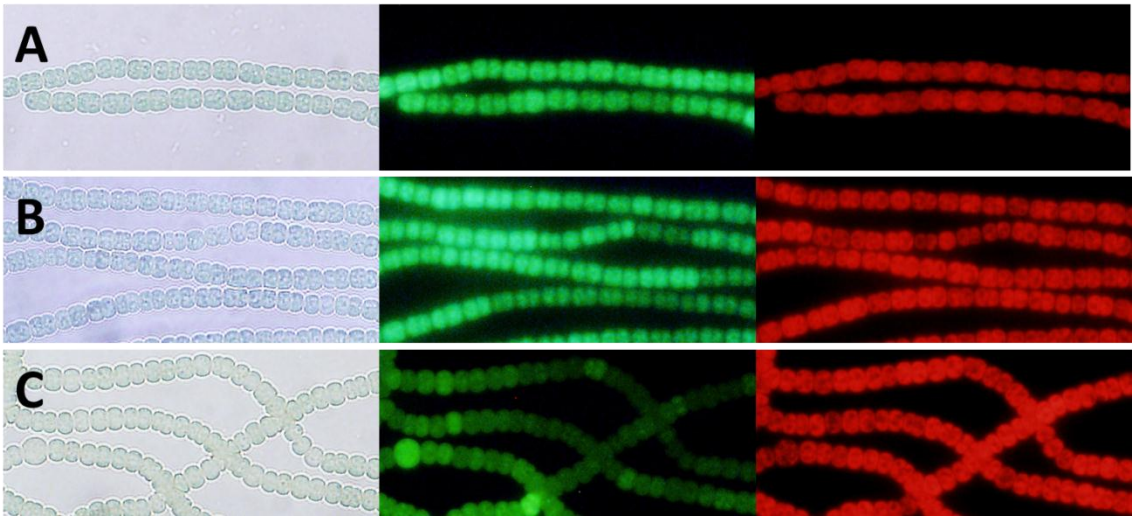

Figure 28: Micrographs (bright field, green fluorescence, autofluorescence) of Δ*hetP*Δ*hetP2* carrying plasmid pKLH101 (P_{hetP3}-GFP) A) 24 hrs, B) 48 hrs, and C) 72 hrs after nitrogen removal.

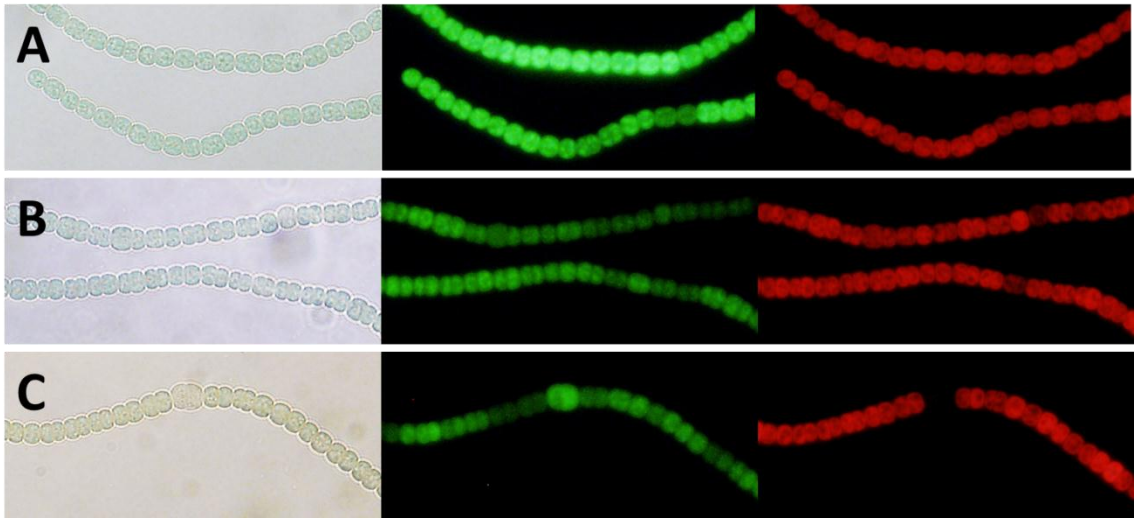

Figure 29: Micrographs (bright field, green fluorescence, autofluorescence) of Δ*hetP*Δ*hetP3* carrying plasmid pKLH101 (P_{hetP3}-GFP) A) 24 hrs, B) 48 hrs, and C) 72 hrs after nitrogen removal.

CHAPTER 5. DISCUSSION

Analysis of the Functional Length of HetP

Truncation mutants of the HetP protein were analyzed on plasmids in a Δ*hetP* mutant strain and in the chromosome to determine the functional length of the HetP protein. Occasionally, heterocyst cells were observed in strains harboring the multi-copy, mobilizable, shuttle vectors encoding the various *hetP* truncation mutants (68, 75, 100, and 125) under the control of the native *hetP* promoter when sampled directly from BG-11 plates with added ammonia. The wild-type strain growing on this type of media does not differentiate heterocysts. This phenomenon may be attributed to the extra copies of the *hetP* promoter associated with these strains. A region within the *hetP* promoter has been shown to partially by-pass the mutant strain *patA*, which typically only differentiates heterocysts at the filament termini; when the *hetP* promoter is overexpressed in a *patA* mutant, intercalary heterocyst cells arise (Higa, 2010).

A similar influence on the production of heterocysts may be occurring in the HetP-truncation strains created with pAM504 based PhetP-$HetP_{truncations}$. Heterocyst cells were not observed in single or double-recombinant HetP-truncation strains grown in BG-11 medium with or without ammonia. However, early onset of pro-heterocysts, when compared to a Δ*hetP* mutant, was observed in the single-recombinant $HetP_{\Delta 26\text{-}159}$ and $HetP_{\Delta 51\text{-}159}$ strains. In the single-recombinant strains, two copies of the *hetP* promoter are present in the chromosome, possibly accounting for the observed phenotype. These early "pro-heterocyst" do not lose auto-fluorescents until 72 hours and although they do stain with Alcian blue at 96 hours, they are phenotypically similar to a Δ*hetP* strain at these later time points. Indeed, in the double-recombinant strains carrying the HetP-25 amino

acid and HetP-50 amino acid truncations, under the control of a single copy of the *hetP* promoter, resemble a Δ*hetP* phenotype (Figure 7).

A $HetP_{\Delta 69\text{-}159}$ strain is capable of forming wild-type percentages of heterocyst cells at 24 hours after nitrogen removal. This 68-amino acid truncation of HetP does not, however, restore a wild-type phenotype. Instead, this strain displays a loss of filament integrity and is thus highly fragmented. The smallest truncated version of the HetP protein that appears to restore a wild-type phenotype, including a wild-type percentage of heterocyst cells, is the strain $HetP_{\Delta 76\text{-}159}$. This mutant encodes the first 75 amino acids of the HetP protein, suggesting at least one functional domain of the HetP protein lies at its amino terminus. This theory is supported by the fact that the transposon in the original transposon screen, used to implicate the role of *hetP* in heterocyt formation, inserted in the region encoding amino acids 50-60 (Fernandez-Pinas, et al. 1994). If the functional size of the HetP protein was smaller than 50 or 60 amino acids, it is likely that the original phenotype of the *hetP*-transposon mutant would not have been characterized as Het- (deficient in producing heterocysts). Two of the three *hetP* homologues were found to functionally complement a Δ*hetP* mutant by 72 hours (Higa, 2010). A BLAST analysis of the amino acid sequence of these homologues to HetP indicates a high sequence similarity in the region of 13-69 amino acids of HetP (Figure 3), further suggesting that the first 75 amino acids are critical to functional role of HetP.

Analysis of the Importance of the Cysteine Residues of HetP

The HetP protein contains two cysteine residues at amino acid residues 36 and 95. Conservative amino acid substitutions of these cysteine residues revealed that the cysteine residue at amino acid 36 is important to the function of the HetP protein. The

roles of these cysteine residues were investigated by introducing conservative cysteine substitutions to a Δ*hetP* mutant strain on replicative plasmids, individually (pPJAV303 and pPJAV304) and in combination (pPJAV305). Mutant strains containing *hetP* with the mutated cysteine residue (conservative substitution to alanine) were also introduced into the chromosome to create the strains $HetP_{C36A}$ and $HetP_{C95A}$ (which were analyzed as single-recombinants). Heterocyst percentages from the resulting strains (plasmid based and chromosomal) were compared and found to be contradictory. The introduction of pPJAV303 (C36A mutation) into a Δ*hetP* background failed to functionally compliment the mutant, as no heterocyst cells were observed at 24 hours after nitrogen removal. The mutant strain, $HetP_{C36A}$ carrying the C to A mutation in the chromosome, did, however, produce heterocyst cells at 24 hours after nitrogen removal. Despite the fact that the chromosomal C36A substitution in the HetP protein produced a near-wild-type percentage of heterocyst, this strain was not capable of growth on nitrogen deficient media. In contrast, both the plasmid-based and chromosomal $HetP_{C95A}$ mutations were capable of functional complementation of a Δ*hetP* strain and were maintained on media lacking a source of fixed nitrogen.

Analysis of the HetP Homologue Mutants

HetP is known to be related to the formation of heterocysts. Originally identified as Het-, the Δ*hetP* mutant was later determined to have a delayed phenotype, ultimately producing 1-2% of heterocyst cells by 72 hours after nitrogen removal. During the investigation of HetP, it was determined that the *Anabaena* genome codes for three homologues of *hetP: hetP1* (*asl1930*), *hetP2* (*alr2902*), and *hetP3* (*alr3234*). Since the amino acids encoded by these genes had a high similarity to the amino acid composition

of HetP, it was conceivable that the delayed phenotype observed in a Δ*hetP* mutant strain was the result of compensation by one or more of the homologues in the absence of *hetP*. To investigate this possibility, each of the homologues were overexpressed in a Δ*hetP* strain, to determine functional complementation. From these experiments, it was determined that *hetP2* and *hetP3* were, at least partially, capable of complementing a Δ*hetP* mutant. Further investigation of this hypothesis required the construction of *hetP*-*hetP* homologue mutants.

Initially, double *hetP*-*hetP* homologue mutants were constructed in order to determine which homologue, if any, might be responsible for the small percentage of heterocyst cells that develop in a Δ*hetP* mutant strain. We hypothesized that at least one of the homologues may be compensating for the loss of *hetP* in the chromosome in a Δ*hetP* strain. However, the resulting strains did not reveal any obvious relationship between *hetP* and any one of its homologues. In fact, all resulting double mutant strains shared a Δ*hetP* phenotype.

No known transcriptional start points (Tsps) of any of the *hetP* homologues have been previously identified. To investigate the expression of each of the homologues, transcriptional reporter constructs were created by fusing the upstream regions of each of the *hetP* homologues to GFP. No expression of GFP was observed in a wild type background containing plasmids carrying the promoter regions of *hetP3* or *hetP2* transcriptionally fused to GFP (pKLH101 and pKLH104, respectively), up to 72 hours after nitrogen removal. This suggests that the *hetP* homologue genes are either not expressed or expressed at very low levels in wild type *Anabaena*. GFP from the transcriptional fusion of *hetP1* (on plasmid pKLH103) was detected slightly above

background levels by 12 hours after nitrogen removal, in the wild type strain. In contrast, strong expression of GFP driven by the promoters of *hetP1* (pKLH103) and *hetP3* (pKLH101) were detected in a Δ*hetP* mutant. It should be noted that expression of GFP from the promoter region of *hetP2* (pKLH104) was never detected in any background strain observed.

Transcription was detected from the promoter regions of *hetP1* and *hetP3* by 0 and 8 hours, respectively, in a Δ*hetP* mutant. This evidence suggests that *hetP* is a possible repressor of both *hetP1* and *hetP3* transcription. Additionally, transcription was detected from each of these constructs in the double mutants Δ*hetP*Δ*hetP1* and Δ*hetP*Δ*hetP3*, suggesting that these genes are not auto-regulated at the level of transcription. Transcription in these strains revealed an increase of expression in heterocyst cells, further supporting the fact that these homologues may play a role in heterocyst function.

With the evidence that the homologues may indeed play some role in heterocyst function, based on the functional-complementation experiments of Δ*hetP*, combinatorial mutants, lacking *hetP* and the various homologues were created. These triple and quadruple mutant strains were further analyzed in hopes to establish a relationship between heterocyst percentages and the *hetP* genes.

The construction of the *hetP* triple mutants revealed that Δ*hetP*Δ*hetP1*Δ*hetP3* failed to grow on media lacking nitrogen. The other *hetP* triple mutants displayed reduced growth on similar media. Not surprisingly, Δ*hetP*Δ*hetP1*Δ*hetP3* heterocysts failed to stain with Alcian blue, suggesting the exopolysaccharide layer of this strain may be deficient. While some cells appear to lose auto-fluorescence, characteristic of

heterocysts, these same cells are often similar in size to vegetative cells and never develop into larger, more round cells typical of mature heterocysts. Finally, this strain was incapable of reducing acetylene in either aerobic or anaerobic atmospheres, suggesting that it is incapable of fixing nitrogen. This is most likely due to the fact that it fails to produce mature heterocysts.

A Δ*hetP* strain has been shown to fix nitrogen, albeit at levels lower than that of wild type, despite its reduced capacity for growth on media lacking nitrogen. This phenomenon has been attributed to the reduced number of heterocysts produced by the strain. The strain Δ*hetP1* was created and determined to differentiate heterocyst cells at wild type levels by 24 hours after nitrogen removal and capable of supporting growth on media lacking a source of fixed nitrogen. A strain lacking *hetP1* and *hetP2*, together, is also capable of fixing nitrogen. Together, these results suggest that *hetP1* is not solely responsible for the phenotype displayed by the triple Δ*hetP*Δ*hetP1*Δ*hetP3* mutant. Single mutant analysis of *hetP3* is required to further investigate the phenotype presented by this strain.

The single mutant strain Δ*hetP2* differentiates a wild type pattern of heterocyst cells by 24 hours after nitrogen removal. Additionally, the heterocyst cells of this strain were shown to stain with Alcian blue and to express FbFP under the control of the *nifB* promoter, on a plasmid. However, no acetylene reduction could be detected from this strain (under aerobic or anaerobic conditions) and it is not capable of supporting growth on media lacking a source of fixed nitrogen, suggesting that the heterocysts formed in Δ*hetP2* are not functional. A strain lacking *hetP2* and *hetP1* (Δ*hetP1*ΔhetP2) differentiates a wild type percentage of heterocyst cells and is capable of supporting

growth on media lacking fixed nitrogen, similarly to a single Δ*hetP1* mutant. This result suggests that *hetP2* is epistatic to *hetP1* and that *hetP1* may be acting antagonistically in regards to the *hetP* alleles. Overexpression of *hetP1* on a plasmid was incapable of functionally complementing a Δ*hetP* mutant (unlike *hetP2* and *hetP3*), thus further supporting the fact that it may have dissimilar function when compared to the other *hetP* alleles.

The triple mutants, Δ*hetP*Δ*hetP1*Δ*hetP2* and Δ*hetP*Δ*hetP2*Δ*hetP3*, were capable of supporting limited growth on solid BG-11_0, although they never differentiated a wild type number of heterocyst cells. Heterocyst cells of these strains appeared smaller than wild type heterocysts and often occurred in multiples. Acetylene reduction assay could not detect any activity under aerobic conditions; however, the strains appear to support at least limited growth on BG-11_0 media, although sustained growth on such media was never observed. Acetylene reduction was detected, albeit at a much lower levels than the control strain, PbP6, under anaerobic conditions. This result suggests that these strains produce functional nitrogenase enzymes at that the heterocyst envelope may not be fully mature. However, due to the fact that these strains can support minimal growth on solid BG-11_0 and reduction of acetylene to ethylene was low under anoxic conditions, it may be wise to repeat the acetylene reduction experiments. Mutant construction and analysis of the single *hetP3* and double Δ*hetP2*Δ*hetP3* strains, is necessary for further analysis of these triple *hetP* homologue mutant strains.

A quadruple *hetP* mutant was created to abolish the function of *hetP* and its homologues, entirely. If a Δ*hetP* mutant was capable of producing a limited number of heterocyst cells due to compensation by one or more of its homologues, it was predicted

that a quadruple *hetP* mutant would be incapable of producing heterocyst cells, altogether. The results were not as predicted. In fact, the *hetP* quadruple mutant actually produced a greater percentage of heterocysts when compared to a Δ*hetP* mutant and all other *hetP*-*hetP*-homologue (double and triple) mutants, although it did not reach wild type levels. The heterocysts of this strain were functional, and shown to reduce acetylene at levels similar to a Δ*hetP* strain. Additionally, the heterocyst were shown to stain with Alcian blue, suggesting their exopolysaccharide layer is intact, and they produced FbFP under the control of the *nifB* promoter, suggesting that at least one of the nitrogenase genes are expressed.

The results of the *hetP* homologue mutant analysis revealed that the relationship between *hetP* and each of its homologues is not as straightforward as originally predicted. Overall, the phenotypes, determined for each of the triple mutants and the quadruple mutant, are dependent upon the rest of the genetic background of the strain. However, there is clear evidence that suggests the *hetP* homologues do play a role in the function of heterocysts. The evidence suggests that the alleles of *hetP* may be controlling the same outputs only in different ways. Further experimentation must be conducted before any conclusions are drawn as to what roles each of the *hetP* homologues play in heterocyst function.

APPENDIX

As described in Chapter 1, it appears that *hetP* plays a role in heterocyst formation in *Anabaena*, based on its delayed heterocyst phenotype. To put *hetP* in context, the role of other genes involved in the cascade of heterocyst differentiation must be further investigated. The current working model for heterocyst differentiation (Figure 2) highlights HetR as a key player in heterocyst formation of *Anabaena* PCC sp. 7120. HetR is considered an activator of heterocyst differentiation and much attention has been devoted to classifying its specific function. HetR has been deemed an activator of heterocyst differentiation where HetN and PatS appear to function as repressors of heterocyst formation. A transcriptional GFP fusion to the promoter region of *hetR* demonstrates that *hetR* is transcribed in all cells. However, translational fusions of GFP fail to produce GFP in any cells, except when expressed in background strains known to have elevated concentrations of HetR (i.e. Δ*patA*)or in strains containing mutant alleles of *hetR* that are not degraded or insensitive to the repressors, HetN and PatS. Thus there appears to be a tight regulation over accumulation of HetR in the wild type strain; important for stoichiometric control over HetR and its influence on heterocyst differentiation. It is known that regions of both HetN and PatS are capable of binding to HetR and can create a gradient of GFP away from heterocysts (viewed in the strains with increased HetR). It is not, however, known how these repressors of heterocysts act on HetR.

To investigate the possibility that the repressors "tag" HetR for degradation by a HetR-specific-protease, YFP translational fusions were made to some known *Anabaena* proteases. These proteases fusions were then introduced to a Δ*patA*Δ*hetFhetR-cfp* with

the purpose of investigating "dual localization" of YFP from the protease with CFP from HetR. HetR fused to GFP has been shown to appear as "puncta" within the cell when exposed to an RGSGR pentapeptide, suspected to be the active portion of both HetN and PatS. Induction of these puncta with *in vitro* addition of RGSGR to Δ*patA*Δ*hetF*H*etR-cfp* proved difficult (only occasional puncta were observed). Specific alleles of HetR, known to demonstrate fluorescence (often appearing as puncta) when translationally fused to GFP, were further investigated for use in the HetR-protease (dual-flourescent-localization) experiments. Plasmids containing a variety of *hetR*$_{mut}$*-cfp* alleles, under the control of the *petE* promoter, were introduced to wild-type, Δ*hetR*, and Δ*patA*Δ*hetR* strains, and observed for the appearance of fluorescent puncta. Chromosomal insertions of the *hetR*$_{mut}$*-cfp* alleles were also attempted. Strains UHM 204 -207 containing the mutant alleles were constructed. Additionally, UHM 208 was constructed to create a Δ*patAhetR*$_{mut}$*-cfp* strain. Unfortunately, no CFP was observed from any of these strains, and creation of additional *hetR-cfp* mutants was halted.

The mutant alleles of *hetR*, investigated for this study, were: HetRC48R, HetRY51C, HetRE56G, HetRQ59P, HetRL161I, HetRP206S, and HetRD230G. These mutant alleles of *hetR* were fused to *gfp* and reported in wild-type and Δ*hetR* backgrounds on plasmids, under the control of the *PetE* promoter. The following tables summarize the results of these promoter fusions:

Table A1: Translational $HetR_{mut}$-GFP fusions viewed in a wild type strain, 0 hrs after nitrogen removal

7120 (wt)	0hrs				
Plasmid	**Plasmid Description**	**Hets +/-**	**GFP**	**Description/Notes**	**Photo**
pSMC232	negative control	het -	No		n/a
pDR293	positive control	het+ MCH	No	highly fragmented/ hets agregated together (clumpy)	n/a
pST193	Y 51 C	het-, pro-hets?	Yes, multiple foci/cell. Seen in almost all cells	descrete puncta- multiple foci/vegetative cells	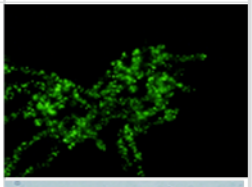
pST194	P 206 S	het+	No	Strain Dead (hard to maintain in culture)/ very sick- light green	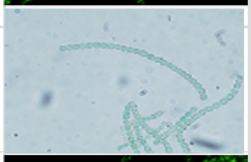
pST195	Q 59 P	het-	Yes. diffuse GFP + multiple foci/cell. GFP visible @ 500ms (strong signal)	<1% hets observed. Filaments highly fragmented and clumped	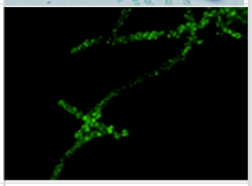
pST196	D 230 G	het+ (more like wt patterning)	Yes. Large puncta in a few vegetative cells (some cells with 2-3 small foci) inconsistancy in GFP/ cell	filaments fragmented/clumped (hets aggregated together)	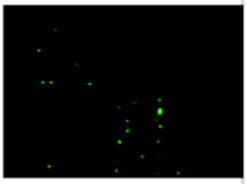
pST197	E 56 G	het+ MCH	yes. Few cells form descrete foci that appear to be elongated	filaments fragmented/clumped (hets aggregated together). Elongated foci appear to be near membrane?	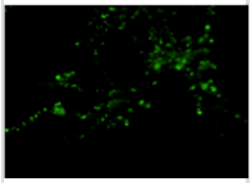
pST198	C 48 R	het-	Yes. Some foci appear elongated	culture unhappy/ cells bleach quickly. Elongated foci near membrane?	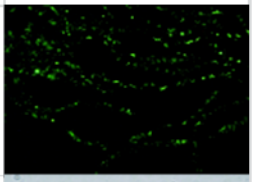
pST199	L 162 I	het+ MCH	No	highly fragmented (5-20 cell filaments), MCH, grows poorly, culture appears "clumpy"	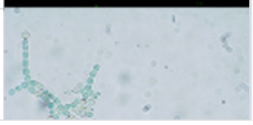

Table A2: Translational $HetR_{mut}$-GFP fusions viewed in a wild type strain, 24 hrs after nitrogen removal

7120 (WT)	24 hr				
Plasmid	**Plasmid Description**	**Hets +/-**	**GFP**	**Description/Notes**	**Photo**
pSMC232	negative control	het +	No		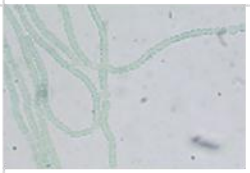
pDR293	positive control	het+ MCH	No	highly fragmented/ hets agregated together (clumpy)	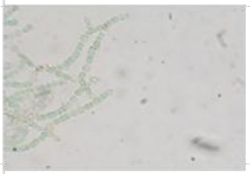
pST193	Y 51 C	het+	Yes. Cresent shaped foci (pattern of flouresence)	GFP does not appear to be present in hets. Culture "clumpy" hets agregated together	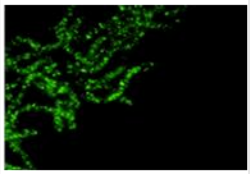
pST194	P 206 S			Strain Dead (hard to maintain in culture)	n/a
pST195	Q 59 P	het+ MCH (lots of pro-hets)	Yes. diffuse GFP, no descrete foci	hets aggregate together (clumpy culture)	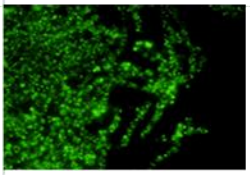
pST196	D 230 G	het+ , abnormal patterning. Some MCH	Yes. Large, descret puncta typically 1/cell occassional cells with multiple (2-3)	Clumpy/fragmented culture- hets aggregate together.	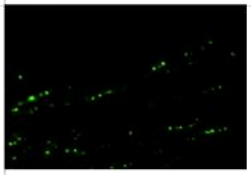
pST197	E 56 G	het+ MCH	yes. A few large foci (cresent shape)	culture is clumpy and highly fragmented as the other cultures. GFP accumulating along periplasm? Exported?	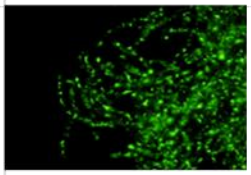
pST198	C 48 R	het+ (lots of pro-hets)	Yes. Cresent foci observed (mostly in dividing cells)	filaments not fragmented- culture is still clumpy- hets aggregating together	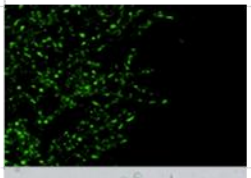
pST199	L 162 I	het+ MCH	No	highly fragmented (5-20 cell filaments), MCH, grows poorly, culture appears "clumpy"	

Table A3: A Translational $HetR_{mut}$-GFP fusions viewed in a wild type strain, 48 hrs after nitrogen removal

7120 (WT)	48hrs				
Plasmid	**Plasmid Description**	**Hets +/-**	**GFP**	**Description/Notes**	**Photo**
pSMC232	negative control	het -	No		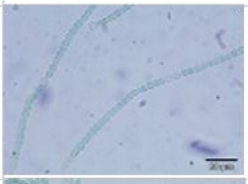
pDR293	positive control	het+ MCH	No		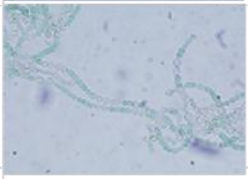
pST193	Y 51 C	het+	Yes, large and small decrete puncta	descrete puncta- multiple foci/vegetative cells	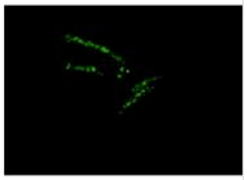
pST194	P 206 S			Strain Dead (hard to maintain in culture)	
pST195	Q 59 P	het+ MCH	Yes. diffuse GFP, no descrete foci	highly fragmented culture	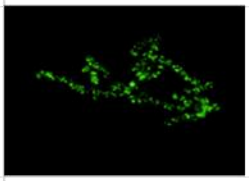
pST196	D 230 G	het+ <2% hets observed/ pro-hets intercilary & terminal	Yes. GFP not consistent throughout filament. Large, single puncta + some cells with multiple small foci.	the larger puncta appear to be forming a "ring" of GFP around the edges of the cells. GFP seems to be forming near poles of cells and at the septa of dividing cells	n/a
pST197	E 56 G	het+ MCH	yes. Descrete foci (large) and some cells with smaller multiple foci	cresent-shaped GFP (puncta?) appear to form. GFP aparent at poles and septa of dividing cells. Not viewed in hets.	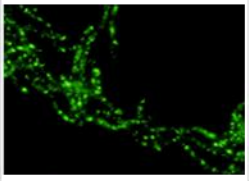
pST198	C 48 R	het+	Yes. 200ms - 1s (very bright) large and small puncta –> multiple/ cell	nice filaments- no clumping observed. .	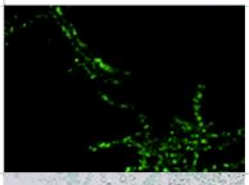
pST199	L 162 I	het+ MCH	No	highly fragmented (5-20 cell filaments), MCH, grows poorly, culture appears "clumpy"	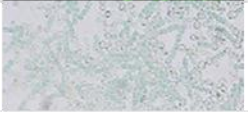

Table A4: Translational $HetR_{mut}$-GFP fusions viewed in a Δ*hetR* strain, 0 hrs after nitrogen removal

ΔR	0hrs				
Plasmid	Plasmid Description	Hets +/-	GFP	Description/Notes	Photo
pSMC232	negative control	het -	No		
pDR293	positive control	het+ MCH	No	highly fragmented/ hets agregated together (clumpy)	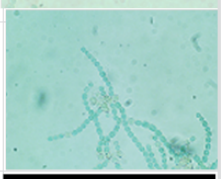
pST193	Y 51 C	het-	Yes, large and small decrete puncta	descrete puncta- multiple foci/vegetative cells/ with some diffuse GFP background	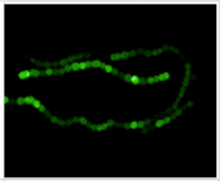
pST194	P 206 S			Strain Dead (hard to maintain in culture)	
pST195	Q 59 P	het-	Yes. diffuse (faint)GFP, no descrete foci	<1% hets observed	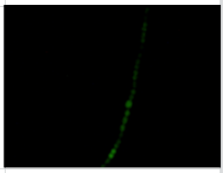
pST196	D 230 G	het+ <2% hets observed/ pro-hets intercilary & terminal	Yes. Large puncta	gfp appears to form a ring (large "puncta" with space in the middle) GFP bright at 200ms. (no visible gfp in hets) puncta appear to be forming at poles and division planes	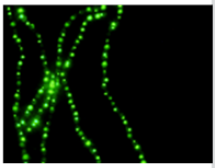
pST197	E 56 G	visable, MCH, abnormal patterning- terminal hets >> intercilary	yes. Descrete foci (large)	appears some cells have multiple foci (small vs large puncta seen is rest of filament) "ring" formation of the GFP observed	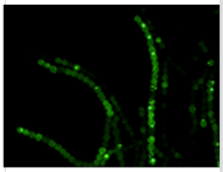
pST198	C 48 R	het-	Yes. 200ms - 1s (very bright) large and small puncta -> multiple/ cell	nice filaments- no clumping observed. 500ms exposure to not "blow out" gfp	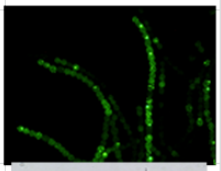
pST199	L 162 I	het+ MCH	No	highly fragmented (5-20 cell filaments), MCH, grows poorly, culture appears "clumpy"	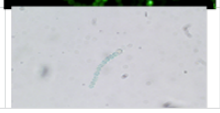

Table A5: Translational $HetR_{mut}$-GFP fusions viewed in a Δ*hetR* strain, 24 hrs after nitrogen removal

ΔR	24 hrs				
Plasmid	Plasmid Description	Hets +/-	GFP	Description/Notes	Photo
pSMC232	negative control	het -	No		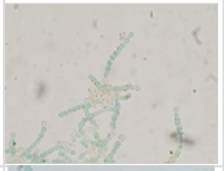
pDR293	positive control	het+ MCH	No	highly fragmented/ hets agregated together (clumpy)	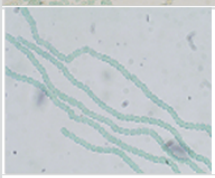
pST193	Y 51 C	het-	Yes, large and small decrete puncta	not consistant throughout the filaments. small and large foci ~1 foci/ cell (@ 24hr GFP weaker than 0hr and 48hr ??	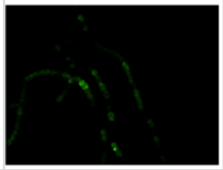
pST194	P 206 S			Strain Dead (hard to maintain in culture)	
pST195	Q 59 P	het- (one pro-het seen in all filaments)	due to culture. Multiple foci/cell small and large with some diffuse GFP throughout filament	cell bleach quickly (N- no hets?) GFP relatively weak compared to other mutHetR-GFP strains	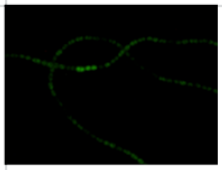
pST196	D 230 G	het+ MCH/ lots of pro-hets	Yes. Large puncta	gfp appears to form a ring (large "puncta" with space in the middle) GFP bright at 200ms. (no visible gfp in hets)	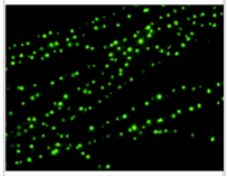
pST197	E 56 G	pro-hets visable, MCH, abnormal patterning- terminal hets >>	yes. Descrete foci (large)	appears some cells have multiple foci (small vs large puncta seen is rest of filament) "ring" formation of the GFP observed	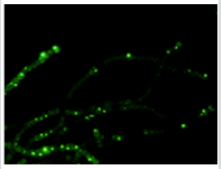
pST198	C 48 R	het-	Yes. Large puncta - appears to be ~1/cell	Puncta appear to form "rings" *not as clear ring formation as pST196).	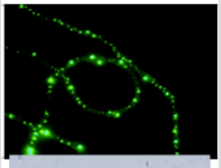
pST199	L 162 I	het+ MCH	No	culture is sickly (N- no hets) lethal? highly fragmented/ hets agregated together (clumpy)	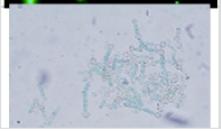

Table A6: Translational $HetR_{mut}$-GFP fusions viewed in a Δ*hetR* strain, 48 hrs after nitrogen remova

ΔR	48 hrs				
Plasmid	Plasmid Description	Hets +/-	GFP	Description/Notes	Photo
pSMC232	negative control	het -	No		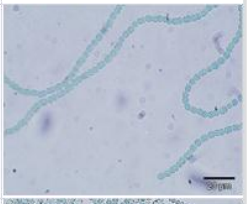
pDR293	positive control	het+ MCH	No	highly fragmented/ hets agregated together (clumpy)	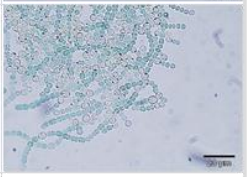
pST193	Y 51 C	het-	Yes, large, decrete puncta	~1 foci/ cell	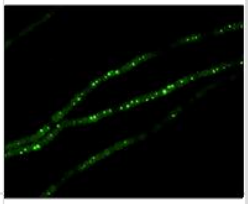
pST194	P 206 S			Strain Dead (hard to maintain in culture)	
pST195	Q 59 P	het+ <1% all terminal	Yes/ mostly diffuse GFP very few descrete foci	few cells with multiple foci/cell	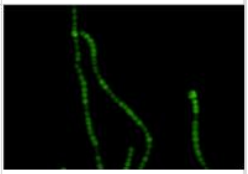
pST196	D 230 G	het+ MCH	Yes. Large puncta	gfp appears to form a ring (large "puncta" with space in the middle) GFP bright at 200ms. (no visible gfp in hets)	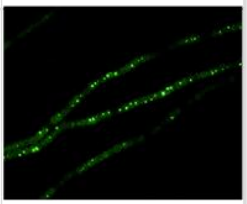
pST197	E 56 G	het+ <2% all terminal	Yes, Large puncta	appears some cells have multiple foci (small vs large puncta seen is rest of filament)	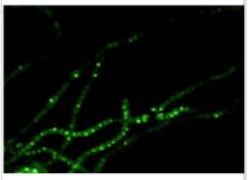
pST198	C 48 R	het-	Yes. Large puncta	Puncta appear to form "rings" *not as clear ring formation as pST196). 1 single (floating) het detected- no GFP	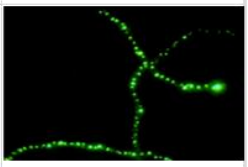
pST199	L 162 I	het+ MCH	No	highly fragmented/ hets agregated together (clumpy)	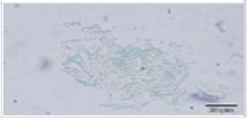

The *Anabaena* genome contains four major classes of proteases: ClpP, Clp ATPases, FtsH, and Lon. The goal of this project was to create C-terminal YFP translational fusions to each of the proteases. Of these 15 proteases, 8 were successfully fused to YFP using the parent, pAM504-based plasmid, pPJAV153; the resultant plasmids are listed in Table A7, bellow. Plasmids were constructed by cloning the coding region of each gene, amplified by PCR, using the primers listed in Table A8, into the BamH1 and Nde1 sites of pPJAV153.

Table A7: *Anabaena* proteases and corresponding YFP-translational plasmids

Protease Family	**Gene**	**Plasmid**
ClpP	*alr 4357*	pKLH107
Clp ATPases	*alr 1963*	pKLH109
	alr 5084	pKLH110
	all 2243	pKLH113
FtsH	*alr 1261*	pKLH115
	all 4936	pKLH116
	all 4476	pKLH117
Lon	*all 4335*	pKLH119

Table A8: Oligonucleotides used to create translational YFP-protease fusion plasmids

Oligonucleotides for YFP-Protease Fusions	Sequence in 5' to 3' Direction
All4357-NdeI-F	AATACATATGCCTATAGGAGGTCTTAAAGTCCCG
All4357-BamHI-R	ATAAGGATCCGACGCGTTCTTCAATCACACGGTC
Alr1963-NdeI-F	AATACATATGTTTGAACACTTCACTTCCGAAGCCATC
Alr1963-BamHI-R	ATTAGGATCCGCCTACATTGGCTAGAAGTAACTCTC
Alr5084-NdeI-F	AATACATATGAAGGCGCTACTGGAACAAGATGG
Alr5084-BamHI-R	AATAGGATCCACTACTAAACACCTCAACAGGTAAGC
All2243-NdeI-F	AATACATATGAGTGATTTATTCAAGGGATTTGAACAG

All2243-BamHI-R	AATAGGATCCATCTGGGCGCTGTTCTGTGAGAAC
Alr1261-NdeI-F	AATACATATGAATAAAAGATGGAGAAATGCGGGG
Alr1261-BamHI-R	ATAAGGATCCGGCAAACGCGGCGGTTTTCACG
All4936-NdeI-F	ATAACATATGCCTGTTGAAACTGATAAAAAAAATTCCATTAAACCACC
All4936-BamHI-R	ATAAGGATCCGACTAGAAGTGTTTGCATTAGGGG
All4476-NdeI-F	ATAACATATGGCAATTTTTGCTAGAAGAATAGGCTTAAATC
All4476-BamHI-R	ATAAGGATCCTTGACTATTAAACCATCGACAATTGCTC
All4335-NdeI-F	ATAACATATGACATCTTCTTCTAGAATTGCCGTCCG
All4335-BamHI-R	ATAAGGATCCTAGCTTTGGATTAAATGTATCT TTCAAAACAG

The translational fusion plasmids were observed in both the wild type and a mutant strain (Δ*patA*Δ*hetFhetR-cfp*) containing HetR translationally fused to CFP (in the chromosome), with the purpose of observing co-localization of fluorescence in the later strain. Although the co-localization portion of the experiment was not performed, YFP was observed in both background strains at 0 hours after nitrogen removal. Of the 8 fusions observed, only three displayed fluorescence, one of which formed discrete foci (similar to those seen in the $HetR_{mut}$-GFP fusions).

Alr5084, Alr4936 and All4335 C-terminal YFP fusions on plasmids pKLH110, pKLH116, and pKLH119, respectively, displayed fluorescence in both wild type and Δ*patA*Δ*hetFhetR-cfp* strains (Figures A1, A2, and A3). Very dim expression, slightly above background levels, of YFP was observed from plasmid pKLH115 (Alr1261-YFP). No expression of YFP was observed in a wild type or Δ*patA*Δ*hetFhetR-cfp* strains harboring plasmids pKLH107 (Alr4357-YFP), pKLH109 (Alr1963-YFP), pKLH113 (All2243-YFP), or pKLH117 (Alr4476-YFP).

In the wild type strain, YFP from plasmid pKLH110 (Alr5084-YFP) was dim when compared to Δ*patA*Δ*hetFhetR-cfp* strain (5 second YFP exposure of 7120 strain vs 2 second YFP exposure of the mutant strain, Fig A1). Most filaments exhibit dull and diffuse YFP with occasional bright foci, when expressed in the wild type. Occasionally, filaments look exactly like the Δ*patA*Δ*hetFhetR-cfp* strain with multiple bright foci in each cell, expressed continuously along the filament (Figure A1).

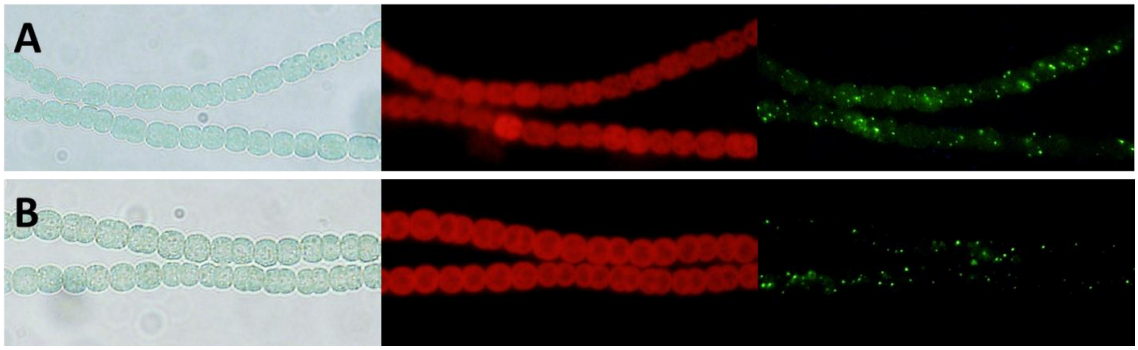

Figure A1: Bright field, autofluorescence, and YFP images of pKLH110 (Alr5084-YFP) in A. 7120 strain (5 second YFP exposure) and B. Δ*patA*Δ*hetFhetR-cfp* (2 second YFP exposure).

Expression of YFP from plasmid pKLH116 (All4936-YFP), fluorescence appears diffuse throughout filament, with occasional, but tiny, foci apparent in some cells (Figure A2). At least one cell in every filament appears much brighter than the neighboring cells.

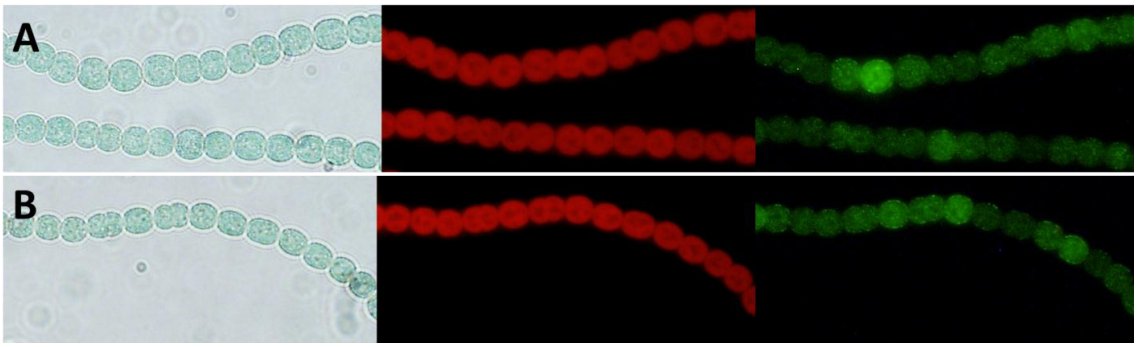

Figure A2: Bright field, autofluorescence, and YFP (5 second exposure) images of pKLH116 (All4936-YFP) in A. 7120 strain and B. Δ*patA*Δ*hetFhetR-cfp*.

Expression from plasmid pKLH119 (All4335-YFP) appeared similar in both the wild-type and Δ*patA*Δ*hetFhetR-cfp* strains. Fluorescence appeared brighter in the Δ*patA*Δ*hetFhetR-cfp* strain. Diffuse fluorescence with small, multiple, foci were observed in each of the cells (Figure A3).

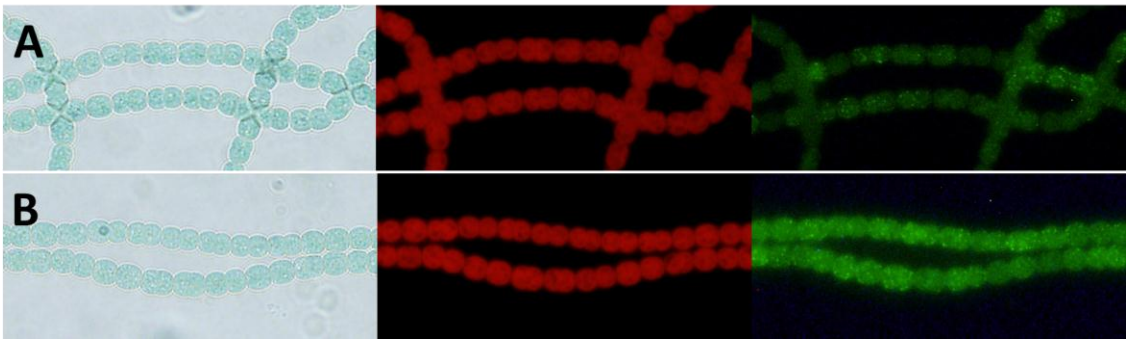

Figure A3: Bright field, autofluorescence, and YFP (5 second exposure) images of pKLH119 (All4335-YFP) in A. 7120 strain and B. Δ*patA*Δ*hetFhetR-cfp*.

REFERENCES

Black, T.A., Cai, Y., and Wolk, C.P. 1993. Spatial expression and autoregulation of *hetR*, a gene involved in the control of heterocyst development in *Anabaena*. Mol. Micro. **9**: 77-84.

Borthakur, P. B., Orozco, C.C., Young-Robbins, S.S., Haselkorn, R., and Callahan, S.M. 2005. Inactivation of *patS* and *hetN* causes lethal levels of heterocyst differentiation in the filamentous cyanobacterium *Anabaena* sp. PCC 7120. Mol. Microbiol. **57:**111-123.

Buikema, W. J., and R. Haselkorn. 1991. Characterization of a gene controlling heterocyst development in the cyanobacterium *Anabaena* 7120. Genes Dev. **5:**321-330.

Buikema, W. J., and R. Haselkorn. 2001. Expression of the *Anabaena hetR* gene from a copper-regulated promoter leads to heterocyst differentiation under repressing conditions. Proc. Natl. Acad. Sci., U.S.A. **98:**2729-2734.

Callahan, S. M. and Buikema, J.W. 2001. The role of HetN in maintenance of the heterocyst pattern in *Anabaena* sp. PCC 7120. Mol. Microbiol. **40**: 941-950.

Cumino A.C., Marcozzi, C., Barreiro, R., Salerno, G.L. 2007. Carbon cycling in Anabaena sp. PCC 7120. Sucrose synthesis in the heterocysts and possible role in nitrogen fixation. Plant Physiol **143**: 1385–1397.

Ernst, A., Black, T., Cai, Y., Panoff, J.M., Tiwari, D.N., and Wolk, C.P. 1992. Synthesis of nitrogenase in mutants of the cyanobacterium *Anabaena* sp. strain PCC 7120 affected in heterocyst development or metabolism. J. Bacteriol. **174:**6025-6032.

Fernandez-Pinas, F., Leganés, F., and Wolk, C.P. 1994. A third genetic locus required for the formation of heterocysts in *Anabaena* sp. strain 7120. J. Bacteriol. **176**(17): 5277-5283.

Gierer, A., and Meinhardt, H. 1972. A Theory of Biological Pattern Formation. Kybernetik. **12:**30-39.

Higa, K. C. 2010. Characterization of the Role of *hetP* in Heterocyst Differentiation in *Anabaena* sp. strain PCC 7120. Master's Thesis. University of Hawaii at Manoa.

Higa, K. C., and Callahan, S. M. 2010. Ectopic expression of hetP can partially bypass the need for *hetR* in heterocyst differentiation by *Anabaena* sp. strain PCC 7120. Molecular Microbiology. **77**: 562-574

Huang, X., Dong, Y., and Xhao, J. 2004. HetR homodimer is a DNA-binding protein required for heterocyst differentiation, and the DNA-binding activity is inhibited by PatS. PNAS. **101**: 4848-4853.

Marcozzi C, Cumino AC, Salerno GL. 2009. Role of NtcA, a cyanobacterial global nitrogen regulator, in the regulation of sucrose metabolism gene expression in Anabaena sp. PCC 7120. Arch Microbiol **191**: 255–263.

Risser, D. D., and S. M. Callahan. 2007. Mutagenesis of *hetR* reveals amino acids necessary for HetR function in the heterocystous cyanobacterium *Anabaena* sp. strain PCC 7120. J. Bacteriol. **189:**2460-2467.

Risser, D. D., and S. M. Callahan. 2009. Genetic and cytological evidence that heterocyst patterning is regulated by inhibitor gradients that promote activator decay. PNAS. **106:**19884-19888.

Thiel T, Pratte B. 2001. Effect on heterocyst differentiation of nitrogen fixation in vegetative cells of the cyanobacterium Anabaena variabilis ATCC 29413. J Bacteriol **183**: 280–286.

Yoon, H.-S., and J. W. Golden. 1998. Heterocyst Pattern Formation Controlled by a Diffusible Peptide. Science. **282:**935-938.

Yoon, H.-S., and J. W. Golden. 2001. PatS and products of nitrogen fixation control heterocyst pattern. J. Bacteriol. **183:**2605-2613.